

Geodynamic significance of a buried transient Carboniferous landscape

Fergus McNab^{1,2,†} and Nicky White^{1,†}

¹Bullard Laboratories, Department of Earth Sciences, University of Cambridge, Madingley Rise, Madingley Road, Cambridge CB3 0EZ, UK

²Helmholtz-Zentrum Potsdam, Deutsches GeoForschungsZentrum (GFZ), Telegrafenberg, 14473 Potsdam, Germany

ABSTRACT

It is increasingly clear that present-day dynamic topography on Earth, which is generated and maintained by mantle convective processes, varies on timescales and length scales on the order of 1–10 m.y. and 10³ km, respectively. A significant implication of this behavior is that Phanerozoic stratigraphic records should contain indirect evidence of these processes. Here, we describe and analyze a well-exposed example of an ancient landscape from the Grand Canyon region of western North America that appears to preserve a transient response to mantle processes. The Surprise Canyon Formation lies close to the Mississippian-Pennsylvanian boundary and crops out as a series of discontinuous lenses and patches that are interpreted as remnants of a westward-draining network of paleovalleys and paleochannels within a coastal embayment. This drainage network is incised into the marine Redwall Limestone whose irregular and karstified upper surface contains many caves and collapse structures. The Surprise Canyon Formation itself consists of coarse imbricated conglomerates, terrestrial plant impressions including *Lepidodendron*, and marine invertebrate fossils. It is overlain by marine, fluvial, and aeolian deposits of the Supai Group. These stratal relationships are indicative of a transient base-level fall whose amplitude and regional extent are recognized as being inconsistent with glacio-eustatic sea-level variation. We propose that this transient event is caused by emplacement and decay of a temperature anomaly within an asthenospheric channel located beneath the lithospheric plate. An analytical model is developed that accounts for the average regional uplift

associated with landscape development and its rapid tectonic subsidence. This model suggests that emplacement and decay of a ~50 °C temperature anomaly within a channel that is 150 ± 50 km thick can account for the observed vertical displacements. Our results are corroborated by detrital zircon studies that support wholesale drainage reorganization at this time and by stratigraphic evidence for spatially variable regional epeirogeny. They are also consistent with an emerging understanding of the temporal and spatial evolution of the lithosphere–asthenosphere boundary.

INTRODUCTION

It is generally accepted that the Earth's surface is deformed by interactions between quasi-rigid tectonic plates. This plate-on-plate lithospheric deformation is dramatically manifest by zones of earthquake seismicity across which relative motion can now be accurately measured by satellite-based surveying. In contrast, the plate tectonic paradigm implies that passive continental margins experience little in the way of vertical motions once plates have rifted and separated. Despite this inference, it is becoming clear that apparently inactive margins located far from plate boundaries can undergo rapid (on the order of 1–10 m.y.) transient vertical motions that appear to be associated with mantle convective dynamics (Moucha et al., 2008; Al-Hajri et al., 2009; Czarnota et al., 2013; Walker et al., 2016). In the North Atlantic Ocean, for example, there is excellent evidence from exposed stratigraphy and calibrated three-dimensional seismic reflection surveys for buried transient landscapes along the fringing passive margins of Greenland and Northwest Europe (Dam, 2002; Shaw Champion et al., 2008; Hartley et al., 2011; Stucky de Quay et al., 2017). These landscapes are not easily accounted for by glacio-eustatic mechanisms and instead their growth and decay are attributed to mantle convective processes. Elsewhere, there is increasing evidence that links intraplate vertical motions with shear-wave velocity anomalies

within the asthenospheric mantle (Phipps Morgan et al., 1995; Richards et al., 2020).

The influence of mantle dynamics on the Earth's surface should be readily apparent throughout the geologic record. One obvious manifestation is intraplate basaltic volcanism, which is often generated by mantle plumes, blobs, and sheets as the consequence of a combination of positive thermal anomalies and thinned lithospheric plates (Wilson and Downes, 2006; McKenzie, 2020; Ball et al., 2021). In principal, the Phanerozoic stratigraphic record should contain indirect information about positive and negative dynamic topography as a function of time and space (White and Lovell, 1997; Petersen et al., 2010). Some progress has been made in identifying and quantifying tectonic subsidence anomalies within sedimentary basins and margins that are attributable to negative dynamic topography (i.e., convective drawdown; Hartley and Allen, 1994; Müller et al., 2000; Czarnota et al., 2013; Morris et al., 2020). However, positive dynamic topography presents a less tractable problem since stratal records of emergent transient landscapes are usually erased by rock removal (Jones et al., 2001).

The Surprise Canyon Formation is exposed throughout the Grand Canyon region of western North America (Fig. 1). It was deposited during late Mississippian times within isolated channels that are incised into shelfal carbonate rocks of the underlying Redwall Limestone, and it is overlain by terrestrial and marine rocks of the Supai Group (Figs. 2A–2D; Billingsley and Beus, 1984; Billingsley and Beus, 1999). These channels are up to 122 m thick, and they are filled with heterogeneous deposits that include conglomerates, sandstones, and limestones (Figs. 2E–2F). Channel bases contain abundant terrestrial flora that are absent from the underlying succession (e.g., *Calamites*, *Lepidodendron*, *Stigmaria*; Billingsley and Beus, 1984; Billingsley et al., 1999). Marine conditions return during deposition of the upper part of the Surprise Canyon Formation and continue into the overlying Supai Group. It has long been recognized that these stratal

Nicky White  <http://orcid.org/0000-0002-4460-299X>

Fergus McNab  <http://orcid.org/0000-0002-8358-1466>

[†]mcnab@gfz-potsdam.de; njw10@cam.ac.uk

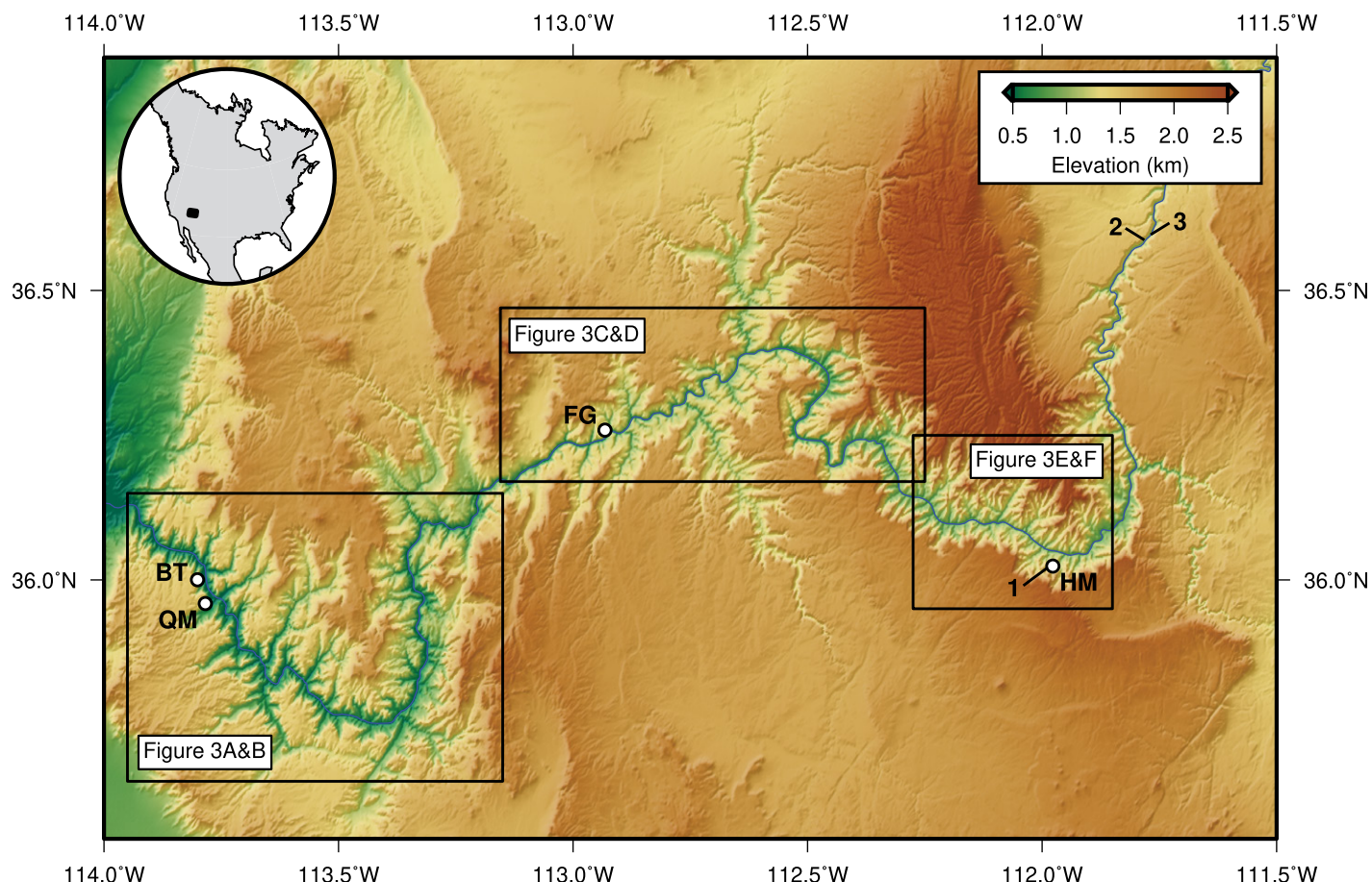


Figure 1. Shaded relief topographic map shows the Grand Canyon region (see inset map of North America). Boxes refer to areas shown in Figure 3. Blue line—Colorado River; white circles—loci referred to in text. BT—Bat Tower; FG—Fern Glen; HM—Horseshoe Mesa; QM—Quartermaster Canyon; numbered lines—loci sampled for detrital zircon analysis by Gehrels et al. (2011), where numbers correspond to those shown in Figure 5.

relationships require an episode of base-level fall, incision, and subsequent resubmergence. Mechanisms that could drive this transient base-level fall include glacio-eustatic sea-level fluctuations and regional tectonic uplift (Billingsley and Beus, 1984; Martin, 1992; Billingsley and Beus, 1999).

Here, we investigate possible causes and consequences of transient base-level fall associated with the Surprise Canyon Formation using a range of approaches. First, we review published stratigraphic and chronologic information relating to the Surprise Canyon Formation, the underlying Redwall Limestone, and the overlying Supai Group. Development of the ephemeral paleolandscape is described and compared with the results of a regional detrital zircon study, with other regional studies, and with the history of Carboniferous glaciation. Secondly, we calculate and analyze the tectonic (i.e., water-loaded) subsidence history of the Grand Canyon region. Finally, a thermal model is developed to account for the

uplift-subsidence excursion associated with growth and decay of this paleolandscape.

STRATIGRAPHIC RELATIONSHIPS

Distributions of exposed Carboniferous rocks throughout the Grand Canyon region are documented in Figure 3. The existence of significant erosional relief at the top of the marine Redwall Limestone has long been recognized, although its significance is debated (Noble, 1922; McKee, 1963; McKee and Gutschick, 1969). Many discontinuous channel-fill deposits were identified and described by Billingsley and McKee (1982) and Billingsley and Beus (1984), who defined the Surprise Canyon Formation as a distinct and mappable rock unit. A series of contributions that are summarized by Billingsley and Beus (1999) described detailed sedimentologic and paleontologic features of this formation (e.g., Shirley, 1988; Grover, 1989; Martin, 1992). Here, we summarize salient observations of the Surprise Canyon

Formation and the lithologies that lie immediately above and below.

Redwall Limestone

The underlying Redwall Limestone is divided into the Whitmore Wash, Thunder Springs, Mooney Falls, and Horseshoe Mesa Members (McKee, 1963; McKee and Gutschick, 1969). The dominant lithologies include bioclastic, pelletal and oolitic limestones, and dolostones with locally abundant chert. These members contain a diverse and definitively marine faunal assemblage that includes foraminifera, corals, bryozoa, cephalopods, crinoids, and rare trilobites (McKee and Gutschick, 1969; Brezinski, 2017). Based on facies variations and disconformities separating each member, a sequence of transgressions and regressions has been identified (McKee and Gutschick, 1969). Kent and Rawson (1980) propose a general shift from earlier open marine to later intratidal conditions.

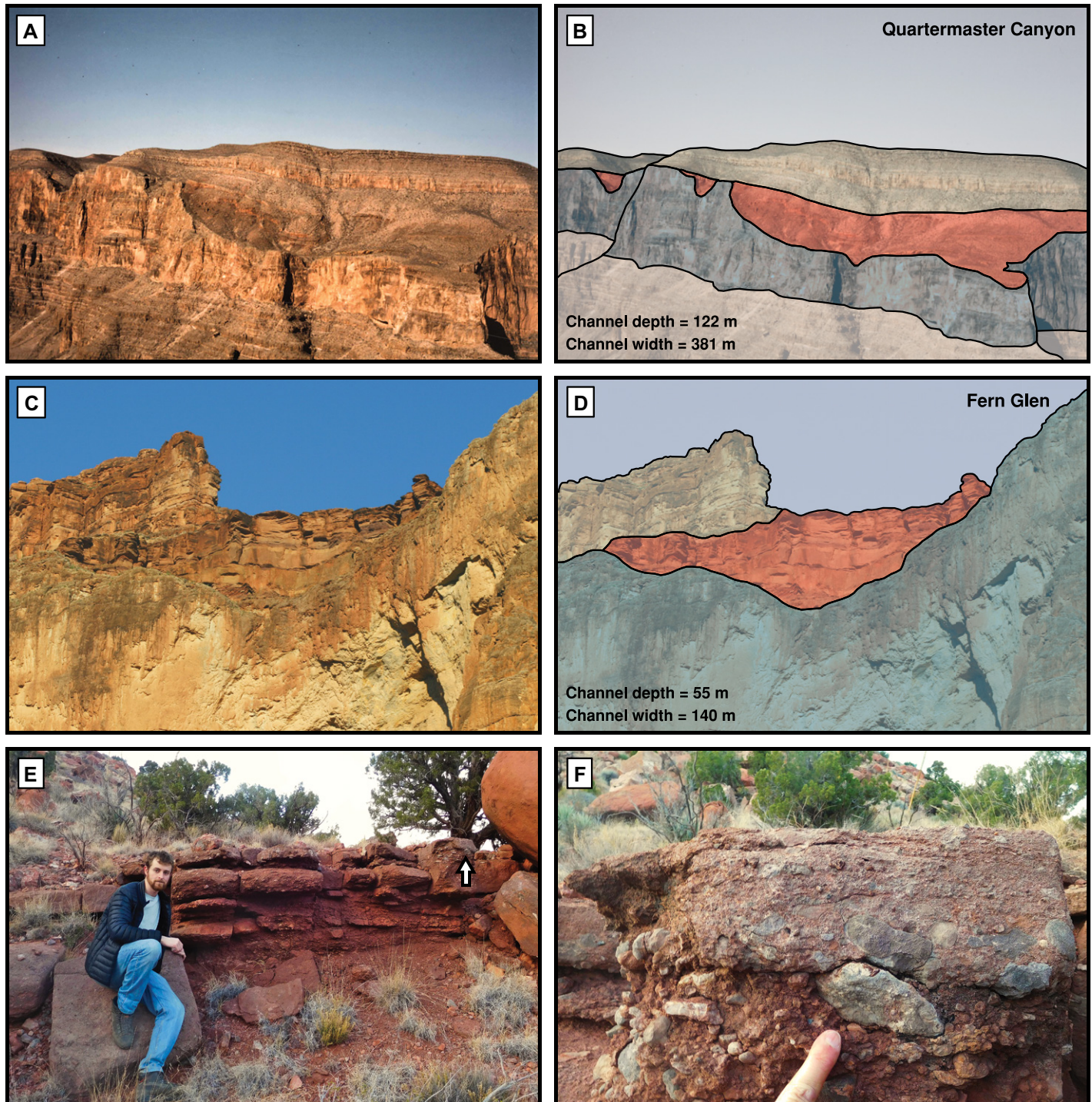


Figure 2. Outcrop examples are shown. (A) Cliff panorama of Surprise Canyon Formation at Quartermaster Canyon (from Grover, 1989). (B) Schematic interpretation of panel A. Dark blue shading—Redwall Limestone; red shading—Surprise Canyon Formation; light blue shading—Supai Group. Channel width and depth measurements are from Billingsley et al. (1999). (C–D) Isolated channel within Surprise Canyon Formation at Fern Glen. Photograph credit: Wayne Ranney. (E–F) Details of channel infill at Horseshoe Mesa. White arrow indicates location of rock face shown in panel F.

Surprise Canyon Formation

The Surprise Canyon Formation itself is divided into three informal units: a lower

conglomerate and sandstone, a middle limestone, and an upper siltstone member (Billingsley and McKee, 1982). Detailed descriptions of outcrops mapped and measured

during field campaigns between 1976 and 1990 are provided by Grover (1989) and Billingsley et al. (1999). A brief summary is provided here.

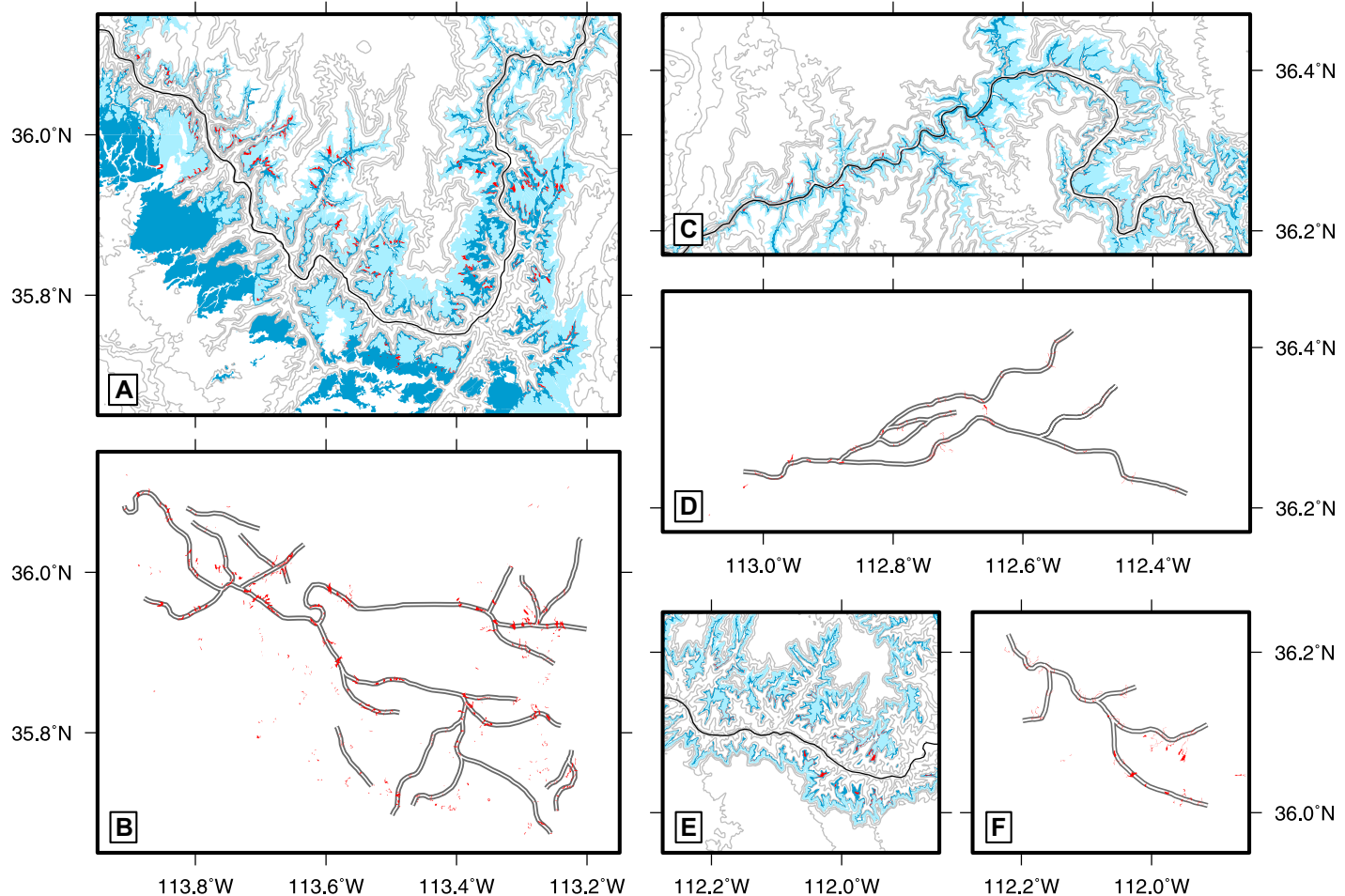


Figure 3. Carboniferous geology of Grand Canyon region is shown. (A) Simplified geologic map of region shown in Figure 1. Dark blue polygons—outcrop distribution of Redwall Limestone; red polygons—outcrop distribution of Surprise Canyon Formation; light blue polygons—outcrop distribution of Supai Group; gray lines—present-day topography contoured at intervals of 200 m; blue line—Colorado River. (B) Outcrop distribution of Surprise Canyon Formation shows paleochannels identified by Grover (1989) and Billingsley (1999). (C–F) Same for other regions specified in Figure 1. Outcrop distributions are based upon Billingsley (2000), Billingsley and Wellmeyer (2003), Billingsley et al. (2006a), Billingsley et al., (2006b), Billingsley et al. (2007), Billingsley et al. (2012), and are available from <http://clark.github.io/grand-canyon-geology> (courtesy of R. Clark).

The lower unit is dominated by pebble to boulder conglomerates and sandstones (Figs. 2E–2F; Grover, 1989; Billingsley et al., 1999). Conglomerate clasts are predominantly made of chert and limestone that are probably derived from the uppermost members of the Redwall Limestone. Sandstones are generally composed of mature quartz arenite. Conglomeratic units are channelized or massive, and the sandstones display a range of sedimentary structures and bedforms, including channelization, cross-stratification, clast imbrication, and small-scale ripples. Paleo-current estimates indicate that westward flow was dominant (Grover, 1989). The sandstone facies also frequently contains lignite, palynomorphs (e.g., spores and pollen grains), carbonaceous plant and wood fragments (e.g., ferns), and *Lepidodendron* impressions (Billingsley and

McKee, 1982; Billingsley and Beus, 1984; Grover, 1989; Billingsley et al., 1999). This evidence suggests that the lower unit was deposited in a terrestrial fluvial environment.

The middle unit is generally represented by a cliff-forming limestone that is separated from the lower unit by an erosional unconformity and contains marine fauna such as foraminifera, corals, cephalopods, and echinoderms (Billingsley and McKee, 1982; Billingsley and Beus, 1984; Grover, 1989; Billingsley et al., 1999). Where present, trough cross-stratification records bimodal paleo-current directions that are dominated by eastward flow. This middle unit is thickest within the western Grand Canyon, thinning and eventually pinching out toward the east (Billingsley et al., 1999). The upper unit mostly consists of siltstones, which are commonly

ripple-laminated and occasionally contain mud-cracks. Contact with the underlying middle unit is gradational. Plant debris and *Lepidodendron* impressions are common (Grover, 1989; Billingsley et al., 1999).

Detailed stratigraphic correlation of discontinuous Surprise Canyon Formation outcrops combined with consideration of paleo-flow directions has enabled reconstruction of a series of westward-draining paleovalleys (Grover, 1989; Billingsley, 1999). This ancient drainage network is shown in Figure 4A with measured channel thicknesses and widths (Fig. 4B; Billingsley, 1999). Channel thicknesses are greatest in the west (i.e., downstream). For example, the Bat Tower and Quartermaster paleovalleys are ~100 m and ~122 m thick, respectively (Fig. 4). Regionally, channel thicknesses

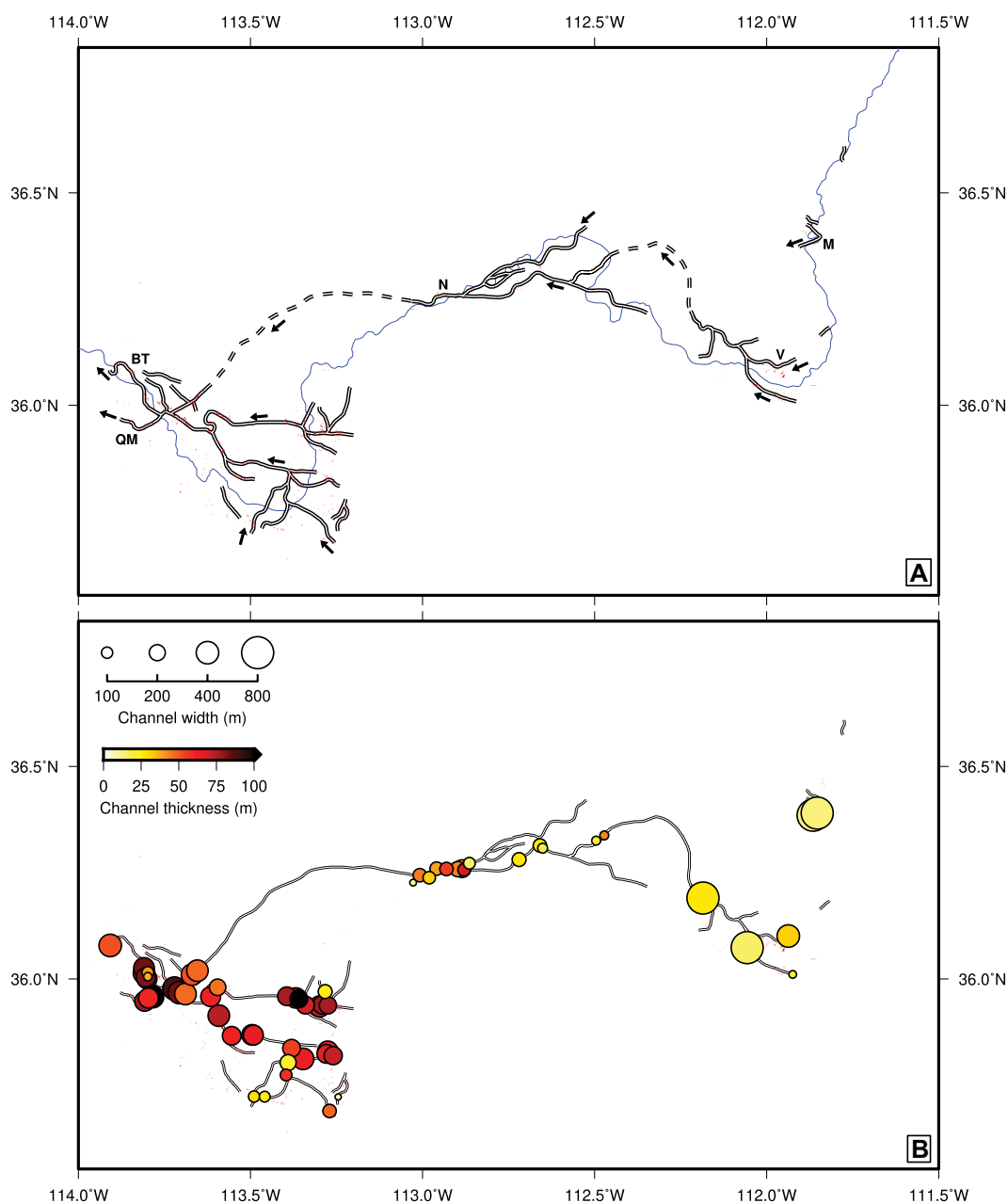


Figure 4. Paleochannels of Surprise Canyon Formation are shown. (A) Reconstructed paleodrainage planform of Surprise Canyon Formation (Grover, 1989; Billingsley, 1999). Small red polygons—outcrop distribution of Surprise Canyon Formation; solid/dashed black lines—inferred/extrapolated paleochannels; black arrows—inferred paleoflow directions; blue line—Colorado River. BT—Bat Tower, M—Marble, N—National, QM—Quartermaster, and V—Vishnu. (B) Outcrop distribution of Surprise Canyon Formation where paleochannel width and thickness measurements are available (Billingsley, 1999). Colored circles—loci of paleochannel measurements where area of circle is proportional to paleochannel width and warmth of color indicates paleochannel thickness (see scale bars); small red polygons—outcrop distribution of Surprise Canyon Formation; black lines—inferred/extrapolated paleochannels.

decrease eastward (i.e., upstream), especially at National paleovalley in the central Grand Canyon, where thicknesses decrease from ~70 m to ~20 m within a few tens of kilometers (Fig. 4). Channel widths are up to ~400 m in the west, and initially they also decrease eastward to <200 m at National paleovalley. However, the greatest channel widths (up to 800 m) are found in the eastern Grand Canyon (e.g., the Vishnu and Marble Canyon paleovalleys; Fig. 4). These channel dimensions are consistent with headward propagation of a wave of incision across an exposed platform such that downstream valleys are broader and deeper. Close to the incising wave front (i.e., around National paleovalley;

Fig. 4), rapid incision produces narrow channels that rapidly shoal onto the preserved platform. Upstream of this incised region, paleovalleys are shallower and less clearly defined.

Although patchy outcrops of the Surprise Canyon Formation are both geometrically variable and compositionally heterogeneous, this general description applies to the majority of the paleovalley network identified by Grover (1989) and Billingsley (1999). One important exception is a sequence of outcrops in the vicinity of Quartermaster Canyon and Burnt Canyon in the western Grand Canyon region (Fig. 4A). In contrast to the mature quartz-arenite sandstones exposed elsewhere, channels in this region contain a

heavy mineral suite that consists of olivines, pyroxenes (including pristine augite crystals), and hornblendes (Grover, 1989, p. 170–173). This mineral assemblage has not been reported from other channels and it also has not been identified within the underlying Redwall Limestone. Since these minerals are expected to rapidly break down during weathering and transportation, it is inferred that there is a local source of coeval mafic volcanism.

Supai Group

The overlying Supai Group is subdivided into the Watahomigi, Manakacha, and Wescogame

Formations that are overlain by the Esplanade Sandstone (McKee, 1975; McKee, 1982). The Watahomigi Formation consists of interbedded mudstones, siltstones, conglomerates, and limestones. The limestones host an abundant marine faunal assemblage that includes foraminifera, bryozoa, and crinoids. In contrast, the mudstones and siltstones contain plant debris and desiccation cracks that are consistent with a nearshore or terrestrial depositional environment. Similar lithologies are found within higher formations along with increasingly predominant cross-bedded aeolian sandstones and occasional evaporitic bodies. Each formation is bounded by channelized erosional unconformities with local relief of up to 30 m that are overlain by basal gravels and conglomerates. The Supai Group is thought to represent a coastal environment in which marine and terrestrial conditions progressively switched in response to a series of transgressions and regressions (McKee, 1982).

In contrast to the Redwall Limestone, which, in the Grand Canyon region, gradually thickens northwestward, the lower formations of the Supai Group appear to have infilled a bathymetric depression known as the Watahomigi Embayment since its expression is most clearly visible within that formation (McKee and Gutschick, 1969; Peirce, 1981; McKee, 1982; Martin, 1992). This embayment is manifest as a ~50-m-thick tongue of marine sedimentary rock that extends in a southwest-northeast direction across the region. Its geometry closely matches the spatial distribution of Surprise Canyon Formation outcrops. It is directly underlain by Surprise Canyon channels that contain marine limestone, while Surprise Canyon channels that contain exclusively terrestrial material lie beneath its margins (Martin, 1992). These stratigraphic observations are consistent with the existence of additional, longer wavelength, erosional relief of at least 50 m at the top of the Redwall Limestone that is not captured by infilled channels of the Surprise Canyon Formation. Rather, this relief appears to have persisted into Supai times as a bathymetric low.

Magnitude of Base-Level Fall

There is excellent stratigraphic evidence that the Surprise Canyon Formation records a period of transient base-level fall that gave rise to emergence, incision, and submergence of the Redwall Limestone. A key question concerns the magnitude of the base-level fall required to account for these stratigraphic observations. An approximate minimum estimate is given by the maximum depth of mapped erosional channels, which is 122 m (Billingsley and Beus, 1999). If the Watahomigi Embayment is taken to reflect

additional erosional relief at the top of the Redwall Limestone, a further ~50 m of base-level fall could be included. However, several lines of evidence suggest that the actual value is probably greater than these minimum bounds.

Sedimentary rocks of the Redwall Limestone, Surprise Canyon Formation, and Supai Group have been buried to significant depths, which implies that they have undergone some degree of compaction. Sclater and Christie (1980) summarize a well-known method for decompacting sediment layers as a function of their composition and burial depth with a view to estimating original depositional thicknesses. At present, Surprise Canyon paleovalleys lie beneath 0.4–1.3 km of younger Paleozoic sedimentary rocks (e.g., Hintze, 1988; Beus and Morales, 2003). Based on apatite fission track thermochronology, Dumitru et al. (1994) estimated that 2.7–4.5 km of Mesozoic strata were subsequently deposited across the Grand Canyon region and later removed. This estimate is consistent with 2.5–3.5 km of coeval strata that are preserved across southern Utah. We infer that Surprise Canyon paleovalleys were buried to depths of 3.1–5.8 km.

The paleovalleys are infilled by a range of lithologies that include sandstone, shale, limestone, and conglomerate, which have different compaction characteristics (see, e.g., Sclater and Christie, 1980; Table 1). Values of the initial porosities and compaction decay lengths for sandstone and shale suggest that a buried (i.e., compacted) channel thickness of 122 m corresponds to an original depositional thickness of ~270 m. If the same channel is filled by limestone, an original depositional thickness of ~190 m is obtained, which can be regarded as a lower bound. The decompact thickness of a given channel probably lies between these end-member estimates. We acknowledge that compaction parameters are subject to considerable uncertainties. For example, both carbonate and orthoconglomeratic units can have significantly lower initial porosities, which will yield smaller original depositional thicknesses. Notwithstanding these uncertainties, limestones and conglomerates typically represent about half of the stratigraphic infill of Surprise Canyon Formation channels, which means that depositional thicknesses of ~200 m are obtained even if limestone

and conglomerate are assumed not to compact. If the Watahomigi Embayment is indicative of additional erosional relief at the top of the Redwall Limestone, depositional thickness estimates could be as great as 260–370 m.

For the purposes of our modeling calculations, we conclude that a reasonable minimum bound for the amount of base-level fall required to account for the stratigraphic relationships is 280 ± 90 m. This estimate still represents a minimum bound for base-level fall that occurred during incision of Redwall Limestone for two reasons. First, shelfal carbonate rocks of the Redwall Limestone were deposited in a shallow marine environment within the euphotic zone (McKee and Gutschick, 1969; Kent and Rawson, 1980). Up to several tens of meters of base-level fall must have occurred prior to any sub-aerial incision to exceed this initial paleobathymetry. Secondly, the contact between the Surprise Canyon Formation and the overlying Supai Group is disconformable (McKee, 1982). This relationship implies that a period of erosion separated deposition of these units and that thicknesses of preserved channels have been reduced by an unknown amount. Additional erosional unconformities occur within sedimentary rocks of the Supai Group that infilled the Watahomigi Embayment. These arguments suggest that base-level fall significantly greater than 200 m is required to fully account for the observed stratigraphic record.

Sediment Provenance and Regional Drainage Patterns

Gehrels et al. (2011) carried out a detrital zircon geochronologic study of the Paleozoic sequence exposed within the Grand Canyon. Zircon grains were collected from sandstone lithologies from each stratigraphic unit and used to determine U-Pb ages and their uncertainties. The resultant suites of U-Pb ages indirectly reflect the age composition of the source region(s) and enable sedimentary provenance to be fingerprinted. In Figure 5, a subset of their results is shown using normalized probability density functions with ages of significant North American sedimentary source regions. For early Paleozoic formations (e.g., Tapeats Sandstone, Bright Angel Shale, Temple Butte),

TABLE 1. LITHOLOGICAL PROPERTIES USED FOR BACKSTRIPPING ANALYSIS

Lithology	Symbol	Initial porosity	Compaction decay length (m^{-1})	Solid grain density ($kg\ m^{-3}$)
Basalt	B	0.1	2500	3000
Dolostone	D	0.2	3000	2860
Limestone	L	0.4	1000	2700
Sandstone	S	0.5	2500	2650
Shale	s	0.6	2000	2700
Salt	X	0.2	750	2160

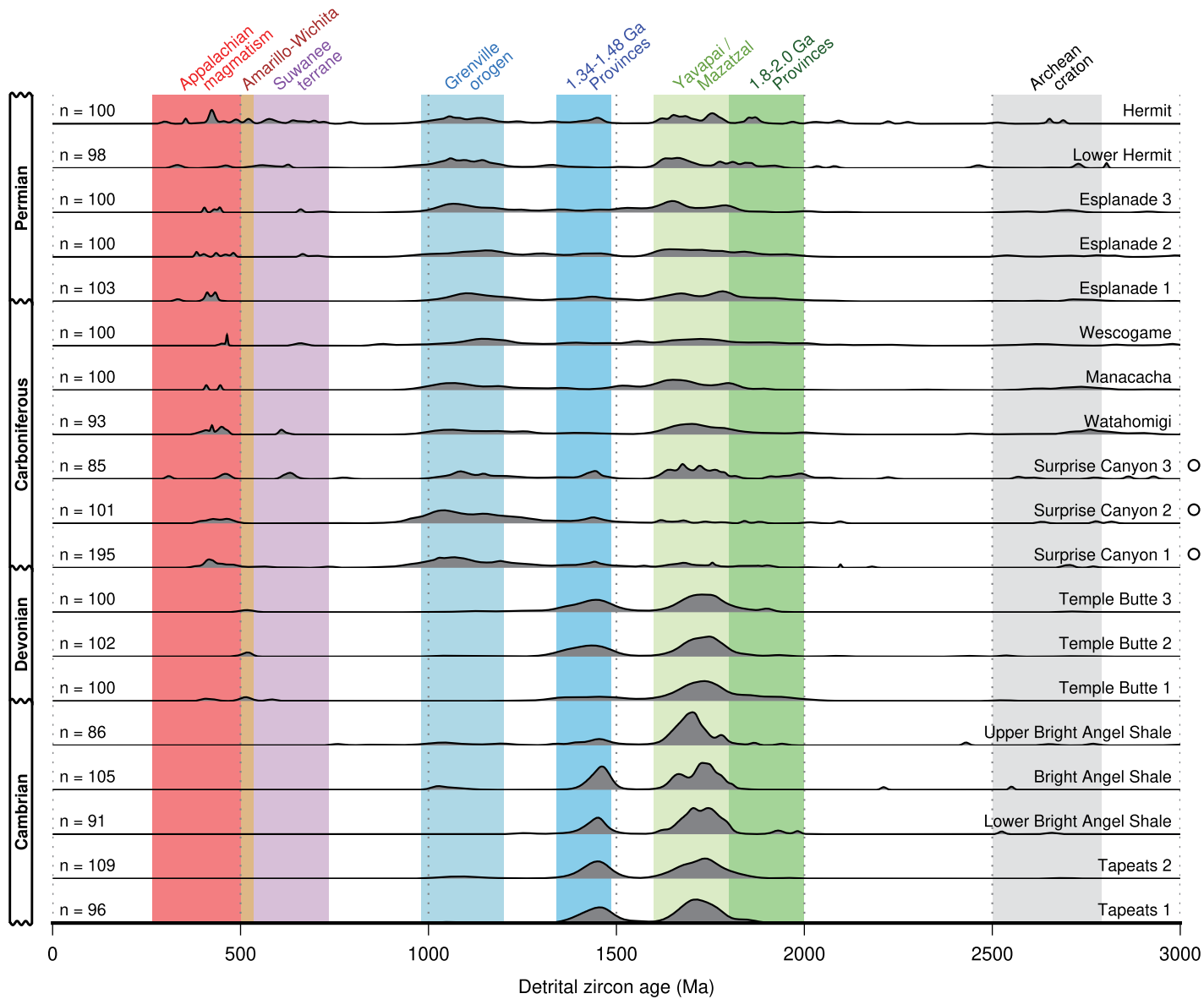


Figure 5. Paleozoic detrital zircon age distributions for the Grand Canyon region are shown. Diagram shows detrital zircon age distributions as a function of lithologic formations within the Grand Canyon region taken from analysis of Gehrels et al. (2011). Horizontal black lines with dark gray fill—normalized probability density functions were generated by combining normal distributions of n calculated U-Pb ages and their uncertainties for each individual formation labeled along the right-hand side where the value of n is given at left-hand side; colored vertical bars represent dominant ages of zircons derived from specific hinterland source regions taken from Gehrels et al. (2011); open circles highlight sub-divisions of Surprise Canyon Formation. See Figure 1 for loci of samples from Surprise Canyon Formation.

a remarkably consistent age distribution was obtained with broad peaks at ca. 1.45 Ga and ca. 1.73 Ga. The source regions of zircon grains with these ages are thought to be the widespread granitic 1.34–1.48 Ga provinces and the Yavapai/Mazatzal provinces, respectively (Anderson and Morrison, 1992; Karlstrom and Bowring, 1993; Gehrels et al., 2011). These sedimentary sources are probably located in central North America east of, and including, the Grand Canyon region and the Transcontinental Arch, a northeast-

southwest-trending topographic high that was exposed during much of the Paleozoic times.

Gehrels et al. (2011) did not sample the Redwall Limestone, which means that there is a ~50 m.y. gap in the detrital zircon record. They did sample the Surprise Canyon Formation at three locations (Fig. 1). Their Sample 1 is from a conglomeratic layer close to the base of this formation in the vicinity of Horseshoe Mesa (Fig. 2). Samples 2 and 3 are from younger sandstone strata located further east. Age dis-

tributions of zircon grains from the lower half of the Surprise Canyon Formation are strikingly different than those from underlying lithologies. For Samples 2 and 3, previously dominant age peaks at ca. 1.45 Ga and ca. 1.73 Ga are now significantly reduced, while a diffuse peak at 1.0–1.3 Ga is emergent. This peak is associated with magmatism of the Grenville orogenic belt of northeastern North America. A smaller cluster of distributed Paleozoic ages (ca. 300–500 Ma) could be associated either with Appalachian

magma or with the Arctic Ellesmerian orogen (Leary et al., 2020). Similar age distributions have been obtained from upper Mississippian channel-fill deposits of Kansas and Arkansas (Wang and Bidgoli, 2019). In the upper Surprise Canyon Formation (i.e., Sample 3) and in younger units, the Grenville peak persists, although it is more subdued and the Yavapai/Mazatzal peak regains its prominence. This distinctive pattern is maintained for the rest of the Paleozoic sequence. Similar results were obtained by Leary et al. (2020) for Pennsylvanian and Permian samples across Arizona.

These dramatic changes in age distributions before and during deposition of the Surprise Canyon Formation probably reflect reorganization of drainage patterns on a regional, if not a continental, scale. Uncertainties in the locations of source regions for the ca. 1.45 Ga and ca. 1.73 Ga peaks that dominated prior to deposition of the Surprise Canyon Formation mean that a detailed understanding of this reorganization and its relationship to Carboniferous base-level fall in the Grand Canyon region is difficult to achieve. A sampling gap of ca. 50 m.y. between the Temple Butte and Surprise Canyon Formations implies that the switch to a Grenville-dominated provenance could conceivably have occurred before deposition of the Surprise Canyon Formation. If Paleozoic grains with ages of 300–500 Ma were sourced from the Appalachian and/or Ellesmerian mountains, the shift to a more easterly and/or northerly source could be a consequence of coeval orogenesis in those regions (Leary et al., 2020). Nonetheless, re-emergence of a significant peak at ca. 1.45 Ga within the upper Surprise Canyon Formation does imply that drainage reorganization was transient and linked to processes that triggered base-level fall and landscape development in the Grand Canyon region.

CHRONOSTRATIGRAPHY AND REGIONAL CONTEXT

A detailed chronostratigraphic framework of Carboniferous rocks from the Grand Canyon region can now be examined. The calibrated timescale and biozone scheme of Davydov et al. (2012) provides a general framework. Additional information relating to foraminiferal, ammonoid, and conodont biostratigraphy is taken from Mamet and Skipp (1970), Ramsbottom and Saunders (1985), Ross and Ross (1988), Lane and Brenckle (2005), and Korn (2006). We also summarize regional stratigraphic correlations and paleogeographic interpretations before comparing the sequence of events from the Grand Canyon region with global glacial reconstructions. The relevant conodont and foraminiferal species reported for Carboniferous rocks of the Grand Canyon and assigned zones and ages are summarized in Table 2 and Figure 6. Regional paleogeographic reconstructions based upon the maps of Poole and Sandberg (1977), Sando (1985), Sando et al. (1990), and Leary et al. (2017) are shown in Figure 7.

Redwall Limestone

Foraminifera and conodonts from the Redwall Limestone are consistent with a middle Tournaisian to middle Viséan age (i.e., ca. 355–337 Ma; Skipp, 1969; Ritter, 1991). During this time, shelfal carbonate deposition is also recorded within the Arrow Canyon sequence of southern Nevada that is located west of the Grand Canyon region (Figs. 6 and 7A). Here, sedimentary rocks of the Monte Cristo Group that include the Anchor Limestone, Bullion, Yellowpine, and lower Battleship Wash Formations were deposited contemporaneously with the Redwall Limestone.

Deposition probably occurred in slightly deeper waters beneath the photic zone, which reflects the more distal position of Arrow Canyon (Bishop et al., 2009). During this period, shelfal carbonate deposition is also recorded within the Madison Limestone of Wyoming, Idaho, and Montana, USA, and within the Leadville Limestone of Utah and Colorado, USA (Fig. 7A; Rose, 1976; Poole and Sandberg, 1977; Gutschick and Sandberg, 1983). Together, these limestones represent a regionally extensive shelfal carbonate platform that developed in shallow seas along a passive margin, which extended roughly north-south across western North America.

East of this platform, deposition ceased along a southwest-northeast trending topographic high known as the Transcontinental Arch (Fig. 7A). West of this platform, a series of flexural basins developed in response to loading related to the Antler orogeny (Fig. 7A; e.g., Poole and Sandberg, 1977; Miller et al., 1992; Giles and Dickinson, 1995). This orogeny is thought to have resulted from arc-continent collision that occurred during closure of the Rheic Ocean and gradual assembly of Pangaea (e.g., Nilsen and Stewart, 1980; Miller et al., 1992; Colpron and Nelson, 2009; Lawton et al., 2017). Paleobathymetry rapidly increased westward into a foreland basin known as the Antler Trough, although Giles and Dickinson (1995) also identify a series of local unconformities across eastern Nevada and western Utah that they relate to development of a flexural forebulge. These unconformities appear to have shifted eastward as the Antler orogen was thrust over the North American craton. In this interpretation, elements of the Redwall-Leadville-Madison carbonate platform may have formed a down-warped, back-bulge basin.

Upper levels of the Leadville and Madison Limestones are marked by prominent karstic surfaces that developed during late Viséan times and are approximately coeval with that observed at the top of the Redwall Limestone (e.g., Sando, 1988; De Voto, 1988; Meyers, 1988). On the Madison Shelf, karst features include enlarged joints, sinkholes, and caves (Sando, 1974; Sando, 1988; Palmer and Palmer, 1995). Maximum relief is up to 60 m, and a westward-flowing fluvial network has been identified. Age estimates for the uppermost Madison Limestone are youngest at the western shelf edge and increase toward the east, which reflects the longer exposure and deeper incision of more proximal stratigraphy (Fig. 6; Sando, 1974; Sando, 1988). Similar observations are described at the Leadville Shelf, where erosional relief of up to 200 m is reported (Maslyn, 1977; De Voto, 1988).

For the more distal Arrow Canyon sequence, carbonate deposition continued until early Serpukhovian times and is represented by the

TABLE 2. CARBONIFEROUS BIOSTRATIGRAPHY OF THE GRAND CANYON REGION

Reported fauna	Zone*	Stage	Age (Ma)
Redwall Limestone			
<u>Base</u>			
Conodonts (Ritter, 1991): <i>Polygnathus communis communis</i> , <i>Pseudopolygnathus multistratus</i> , <i>P. oxyptageus</i> , <i>P. nudus</i> .	Mc7	Tournaisian–	353–
Foraminifera (Skipp, 1969): <i>Septaglomospirina primaeva</i> , <i>Tuberendothyra tuberculata</i> .	Mf6		
Top			
Foraminifera (Skipp, 1969): <i>Endothyra scitula</i> , <i>E. pauciseptata</i> .	Mf11	–Viséan	–337
Surprise Canyon Formation			
Conodonts (Grover, 1989; Martin, 1992; Martin and Barrick, 1999): <i>Adetognathus unicornis</i> , <i>A. spathus</i> , <i>A. laetus</i> , <i>A. gigantus</i> , <i>Cavusgnathus navicularis</i> , <i>C. unicornis</i> , <i>Gnathodus billineatus</i> , <i>Rachistognathus muricatus</i> , <i>R. primus</i> .	Mc16	Serpukhovian	327–
Foraminifera (Martin, 1992; Billingsley and McKee, 1982; Beus and Martin, 1999): <i>Eosigmolina explicate</i> , <i>E. rugosa</i> , <i>E. robertsoni</i> , or <i>Brenckleina rugosa</i> .	Mf18		–325
Watahmi (Supai Group)			
<u>Base</u>			
Conodonts (Martin, 1992; McKee, 1982): <i>Adetognathus laetus</i> , <i>A. spathus</i> , <i>Rachistognathus muricatus</i> , <i>R. websteri</i> , <i>R. proxilus</i> .	Mc17	Bashkirian–	323–
Foraminifera (McKee, 1982): <i>Astroarchaeodiscus</i> sp.		–Moscovian?	–310

*From global correlation of the Carboniferous time scale and biozones of Davydov et al. (2012).

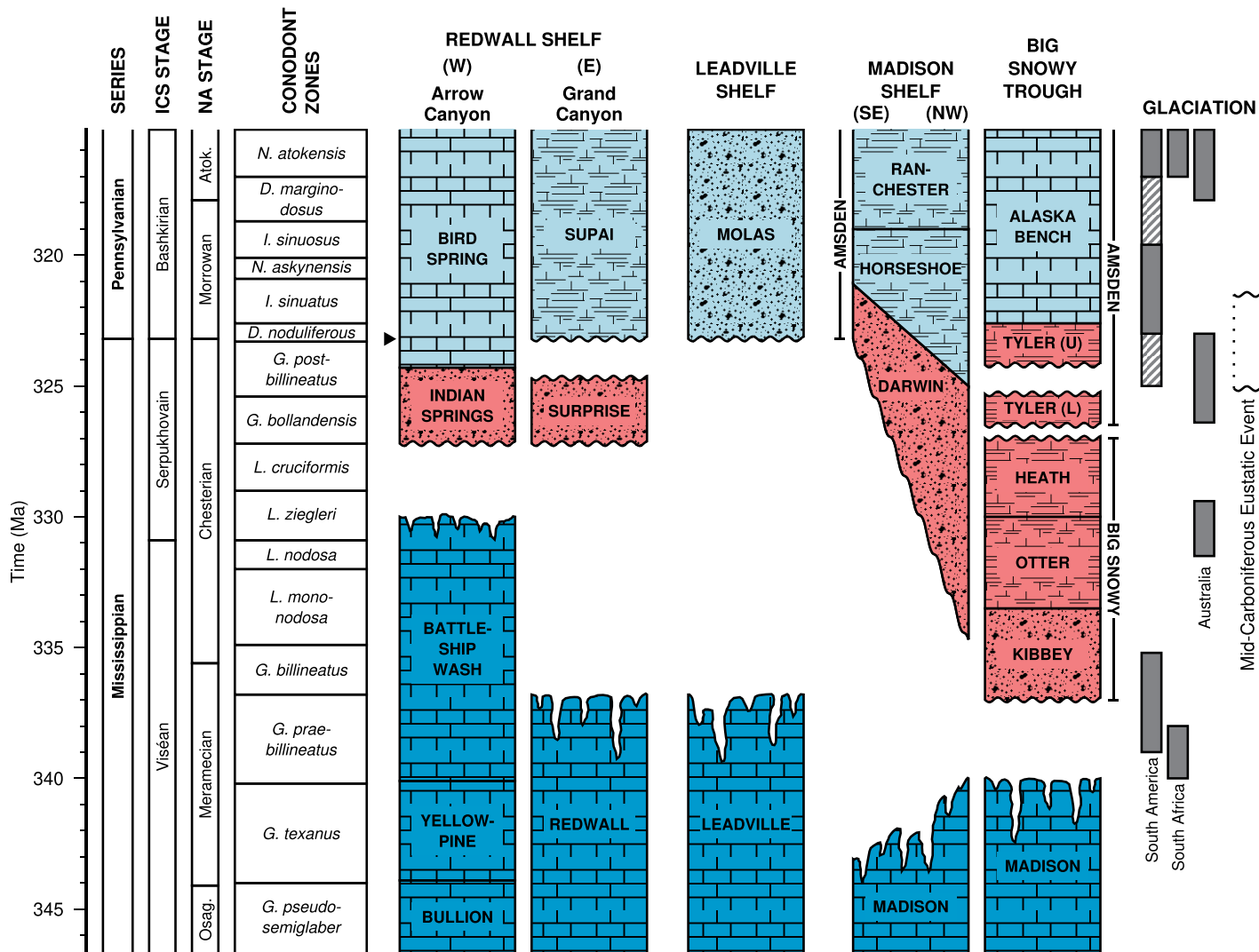


Figure 6. Carboniferous chronology of the Grand Canyon and surrounding regions is shown. Columns at left-hand side summarize chronostratigraphy and biostratigraphy of Mississippian and Pennsylvanian units. Dark blue polygons with brick pattern—Redwall Limestone and other correlative units (irregular top surfaces indicate karstification); red polygons with clastic/semi-brick patterns—Surprise Canyon Formation and correlative units; light blue polygons with clastic/brick/semi-brick patterns—Supai Group of formations and correlative units; solid/wiggly lines—conformable/disconformable stratigraphic boundaries; solid arrow head—locus of global boundary stratotype (Lane et al., 1999); gray/hatched vertical bars along right-hand side summarize continental probable/possible glaciation records (Montañez and Poulsen, 2013). Mid-Carboniferous eustatic event defined by Ramsbottom and Saunders (1985) on timescale of Davydov et al. (2012) is shown. See Table 2 and Figure 7 for further details and locations.

Battleship Wash Formation. Bishop et al. (2009) suggest that bathymetry shallowed during this period and culminated in a depositional hiatus represented by paleosol development. Saltzman (2003) and Dyer et al. (2015) identify a coincident negative perturbation of $\delta^{13}\text{C}$, which they link to weathering of the exposed proximal carbonate platform.

Surprise Canyon Formation

Conodonts (e.g., *Adeotognathus unicornis*) restrict the Surprise Canyon Formation to the

middle Serpukhovian stage (Table 2; Fig. 6; Martin, 1992; Martin and Barrick, 1999). This chronology, which is consistent with the floral assemblage described by Tidwell et al. (1992) and with brachiopod fauna identified by Beus (1999) and Beus and Martin (1999), implies that there is a <10 m.y. period of landscape development between the top of the Redwall Limestone and deposition of the Surprise Canyon Formation. Deposition then lasted up to ~3 m.y. and overlaps with deposition of the Indian Springs Formation at Arrow Canyon during middle to late Serpukhovian times. The Indian Springs

Formation consists of limestones and shales, but it also contains several paleosol deposits that represent episodes of sub-aerial exposure and weathering (Bishop et al., 2009). These particular discontinuities do not appear to be associated with significant erosional relief.

No sedimentary rocks of Serpukhovian age have been identified above the Leadville Limestone, but on the Madison Shelf, deposition of the Amsden Formation, which overlies the Madison Limestone, does appear to coincide with that of the Surprise Canyon Formation (Fig. 6; Sando et al., 1975). The lowermost Darwin

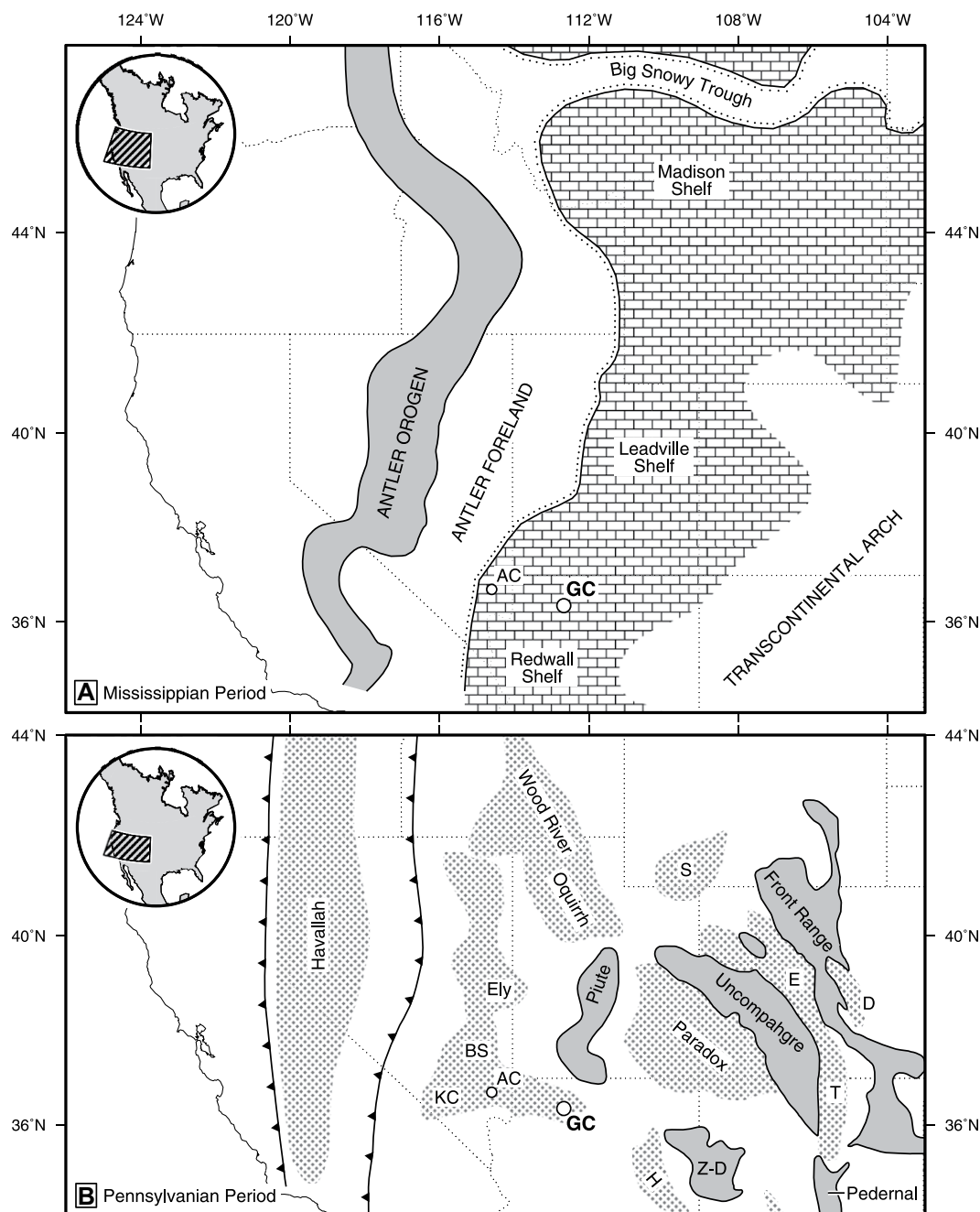


Figure 7. Carboniferous paleogeography of western North America is shown. (A) Paleogeographic reconstruction of western North America during Mississippian times is based upon Poole and Sandberg (1977), Sando (1985), and Sando et al. (1990). Brick pattern—carbonate deposition on cratonic platform; AC—Arrow Canyon; GC—Grand Canyon; gray polygon—locus of Antler orogen. Inset map shows regional location. (B) Paleogeographic reconstruction of western North America during Pennsylvanian times is based upon Leary et al. (2017). Gray polygons—loci of uplifted Ancestral Rocky Mountains. Z-D—Zuni-Defiance zone; stippled polygons—sedimentary basins/troughs; GC—Grand Canyon; AC—Arrow Canyon; KC—Keeler Canyon; BS—Bird Spring; S—Sweetwater; E—Eagle; D—Denver; T—Taos; and H—Holbrook. Note that locations are approximate since they are based on present-day outcrop distributions that have been affected by Mesozoic and Cenozoic deformation. Inset map shows slightly smaller regional location than in panel A.

Sandstone Member of this formation consists of conglomerates and sandstones that were probably deposited in a fluvial to coastal setting. Mirroring distribution of the Madison Limestone, the Amsden Formation thins and youngs from west to east, which is once again consistent with progressive eastward marine transgression (Sando et al., 1975; Sando, 1988). In the more distal Big Snowy Trough, terrestrial sandstones of the Kibbey Formation (i.e., Big Snowy Group) overlie karstic surfaces at the top of the Madison Limestone (Maughan and Roberts, 1967; Ahern and Fielding, 2019). A return to marine

deposition is recorded by limestones and shales of the overlying Otter and Heath Formations. Unconformities and conglomeratic deposits in the subsequent Tyler Formation probably record further base-level fluctuations near the Mississippian-Pennsylvanian boundary (Maughan, 1984; Singer et al., 2019). It is worth noting that deposition of the lowermost supra-karstic Amsden and Kibbey Formations during late Viséan times appears to overlap with deposition of the sub-karstic Battleship Wash Formation at Arrow Canyon. This temporal relationship implies that transient base-level fall affected the more north-

ern Madison Shelf slightly earlier than the Redwall Shelf of the Grand Canyon region (Fig. 6).

Supai Group

The Watahomigi Formation at the base of this group contains a conodont assemblage that is consistent with a latest Serpukhovian or earliest Bashkirian age. The diagnostic *Declinognathodus noduliferous* of early Bashkirian times is reported several meters above the base (Table 2; Fig. 6; McKee, 1982; Martin, 1992). This age implies that a hiatus of up to ~2 m.y. occurred

between deposition of the Surprise Canyon Formation and the onset of deposition of the Supai Group. Deposition continued until Early Permian times (McKee, 1982). The Supai Group correlates with the Bird Spring Formation at Arrow Canyon (Lane et al., 1999; Bishop et al., 2009; Bishop et al., 2010). This formation lies conformably on top of the Indian Springs Formation and mostly consists of sands and carbonates deposited within a shelfal setting. Thin conglomeratic units with erosional bases also occur. The Bird Spring Formation contains the global boundary stratotype point for the Serpukhovian-Bashkirian (i.e., Mississippian-Pennsylvanian) boundary, which is fixed at a height of 7.6 m above its base (Fig. 6; Lane et al., 1999).

During this period, western North America became influenced by the collision of Gondwana and Laurentia along the Marathon-Ouchita-Appalachian suture located southeast of the Grand Canyon region. Together with a left-lateral transpressional boundary located to the southwest, this collision generated a complex pattern of intraplate deformation that resulted in the growth of a series of basement-cored uplifts known as the Ancestral Rocky Mountains (Fig. 7B; e.g., Kluth and Coney, 1981; Dickinson and Lawton 2003; Leary et al., 2017). Examples in the vicinity of the Grand Canyon region include the Uncompahgre and Zuni-Defiance Uplifts. Foreland basins such as the Paradox and Holbrook basins developed alongside these mountain ranges (Fig. 7B; e.g., Barbeau, 2003; Dickinson and Lawton, 2003; Sturmer et al., 2018).

Glacio-Eustatic Sea-Level Fluctuations

A possible mechanism for generating the base-level fall associated with the Surprise Canyon Formation is eustatic sea-level change, since the Carboniferous period was a time of extensive glaciation (e.g., Ross and Ross, 1985; Veevers and Powell, 1987; Fielding et al., 2008). Two key questions are whether a global eustatic event can be shown to coincide with regional incision of the Redwall Limestone and with deposition of the Surprise Canyon Formation and whether Carboniferous glacio-eustasy can generate observed base-level fall of at least 200 m.

The precise nature of late Paleozoic glaciation is much debated. Reconstructions are generally based on three closely related sets of observations: the distribution of glacial deposits, particularly across southern Gondwana, which was positioned near the South Pole (i.e., present-day Antarctica, South America, southern Africa, and Australia); relative sea-level variations observed in far-field sedimentary basins (e.g., present-day North America and Eurasia); and geochemical

proxies across stratigraphic boundaries. Veevers and Powell (1987) favor brief phases of glaciation in Late Devonian and Viséan times followed by major and protracted glaciation that initiated in Serpukhovian times and lasted until Early Permian times. Subsequently, it has instead been argued that this major and protracted period of glaciation can be sub-divided into a series of distinct, shorter glaciations (e.g., Fielding et al., 2008; Montañez and Poulsen, 2013). In particular, the growth of small, localized ice depocenters may have started during middle Viséan to Serpukhovian times and been followed by an increase in ice volume and extent toward the start of the Bashkirian stage (Fig. 6). This revised chronology is broadly consistent with $\delta^{18}\text{O}$ values that increase through Serpukhovian times into early Bashkirian times (Mii et al., 1999; Mii et al., 2001; Grossman et al., 2008). In general, Carboniferous ice sheets are thought to have remained relatively localized in contrast to the extensive ice sheets that have developed, for example, in Neogene and Quaternary times (Montañez and Poulsen, 2013). Simulations of late Paleozoic glaciations suggest that, to maintain localized ice sheets, ice volumes equivalent to eustatic sea-level falls of <50 m are required (Horton et al., 2010, 2012).

Saunders and Ramsbottom (1986) compared stratigraphic sections from North America, northern Africa, and Eurasia. They identify a ubiquitous and prominent unconformity during middle Carboniferous times, which they call the “mid-Carboniferous eustatic event.” This event is defined using ammonoid zones and starts with the top part of the *Eumorphoceras* zone (“E_{2c}”) and lasts until the lowest part of the *Reticuloceras* zone (“R₁”), though the precise timing and duration of this hiatus varies by location. These zones correspond to an upper Serpukhovian to lower Bashkirian age and span the Mississippian-Pennsylvanian boundary (Fig. 6; Ramsbottom and Saunders, 1985; Korn, 2006; Davydov et al., 2012). Saunders and Ramsbottom (1986) highlight conglomeratic beds and short-lived hiatuses within the Indian Springs and Bird Spring Formations at Arrow Canyon, which they associated with the onset and termination of this event, respectively. The eustatic event has also been linked to development of a transient landscape in the central Appalachian basin (Beuthin, 1994; Blake and Beuthin, 2008). Here, marine limestones, shales, and sandstones of the Serpukhovian Mauch Chunk Group and Bluestone Formation are incised and overlain by sandstones of the New River and Pocahontas Formations. A set of southwestward-draining paleovalleys has been identified that runs parallel to the Appalachian range front and extends across Virginia, Kentucky, Indiana, Illinois, and Arkansas

(Siever, 1951; Bristol and Howard, 1971; Rice, 1984, 1985; Howard and Whitaker, 1988; Droste and Keller, 1989; Beuthin, 1994; Webb, 1994; Archer and Greb, 1995). Local relief of up to ~100 m is reported, although the amplitude of base-level fall may have been locally amplified by flexural uplift (e.g., Ettensohn, 1994).

In the Grand Canyon region, incision of the Redwall Limestone begins in middle Viséan times and continues until middle Serpukhovian times, when deposition of the Surprise Canyon Formation began (Fig. 6). At the more distal Arrow Canyon section, this depositional hiatus was delayed until early Serpukhovian times. Base-level fall and incision of the Redwall Shelf appears to correlate with the onset of localized glaciation in middle Viséan to early Serpukhovian times (e.g., Veevers and Powell, 1987; Fielding et al., 2008; Montañez and Poulsen, 2013). Even though base-level fall in the Grand Canyon region appears to have ended with resumption of deposition during middle Serpukhovian times (represented by the Surprise Canyon and Indian Springs Formations), ice-sheet growth is considered to have reached its maximum extent in late Serpukhovian to early Bashkirian times (Veevers and Powell, 1987; Fielding et al., 2008; Montañez and Poulsen., 2013). On the Redwall Shelf, disconformities between the Surprise Canyon Formation and Supai Group and within the Indian Springs and Bird Spring Formations occur at this time, coeval with development of the globally recognized middle Carboniferous unconformity identified by Saunders and Ramsbottom (1986).

While ice-sheet histories, isotopic records, and the presence of a globally recognized unconformity are consistent with peak ice-sheet extent and a coeval eustatic sea-level lowstand close to the Mississippian-Pennsylvanian boundary, its manifestation within the Grand Canyon region is weak compared with the dramatic early Serpukhovian base-level fall recorded by the Surprise Canyon Formation itself. Uncertainties in ice-sheet reconstructions and in the correlation of deposits require that these interpretations be made with a degree of caution. We emphasize that, regardless of the precise timing of events, an observed base-level fall of at least ~200 m is considerably larger than typical estimates of Carboniferous sea-level fluctuations (i.e., ~50 m; Horton et al., 2010, 2012; Montañez and Poulsen., 2013). Existing reconstructions of late Paleozoic glaciation are therefore inconsistent with both the magnitude and, it would appear, the timing of observed incision of the Redwall Limestone and the development of paleovalleys preserved within the Surprise Canyon Formation. Instead, a period of transient regional uplift is deemed necessary.

TECTONIC SUBSIDENCE ANALYSIS

Subsidence calculations play a significant role in elucidating the tectonic mechanisms that generate sedimentary basins and margins (e.g., Sleep, 1971; Steckler and Watts, 1978). Here, we present and analyze a tectonic (i.e., water-loaded) subsidence history of the Grand Canyon region with a view to developing an understanding of the causes and consequences of transient landscape development during Carboniferous times. The average subsidence history from Proterozoic to late Paleozoic times is reconstructed using stratigraphic measurements given by Hintze (1988) and Beus and Morales (2003) and summarized in Table 3. A revised chronologic framework for the Proterozoic Unkar and Chuar

Groups, and the Cambrian Sixtymile Formation and Tonto Group, is used (Weil et al., 2003; Timmons et al., 2005; Timmons et al., 2012; Dehler et al., 2017; Rooney et al., 2018; Karlstrom et al., 2018). The uncorrected subsidence curve calculated from these sedimentary thicknesses is shown in Figure 8A. These observed measurements are backstripped and unloaded to correct for the effects of compaction and sedimentary infill following the well-known procedure described by Steckler and Watts (1978) and Sclater and Christie (1980). It is important to correct for paleobathymetric changes as a function of time. The assumed values of initial porosity, compaction decay length, solid grain density, and paleobathymetry are summarized in Tables 1 and 3. The resultant water-loaded subsidence curve

illustrates the growth of water-loaded accommodation space as a function of time (Fig. 8B).

Tectonic subsidence recorded by sedimentary strata exposed in the Grand Canyon is strongly episodic and typical of cratonic regions. The oldest preserved subsidence event occurred during Mesoproterozoic times and is represented by the Unkar Group (1255–1100 Ma). During this period, rapid, nonlinear tectonic subsidence occurs which, combined with observational evidence for syn-sedimentary monoclinal structures in the lower half of this sequence, is regarded as being consistent with deposition within a foreland basin setting associated with the Grenville orogen and the assembly of Rodinia (Timmons et al., 2005; Timmons et al., 2012; Mulder et al., 2017). Upper sequences of the Unkar Group are

TABLE 3. STRATIGRAPHIC INFORMATION FROM THE GRAND CANYON REGION USED FOR BACKSTRIPPING ANALYSIS

Formation	Age (Ma)	Thickness (m)	Lithology*	Environment†	Water depth† (m)	References
<u>Unkar Group</u>						
Bass Limestone	1255–1187	57–100	DDDS	Shallow marine, tidal	0–40	Hendricks and Stevenson (2003), Timmons et al. (2005)
Hakatai Shale	1187–1167	135–300	Ssss	Mudflat, shallow marine	0–40	Hendricks and Stevenson (2003), Timmons et al. (2005)
Shinumo Quartzite	1167–1140	345–405	SSSS	Fluvial, deltaic	0–40	Hendricks and Stevenson (2003), Timmons et al. (2005)
Escalante Creek	1140–	390	SSSs	Shallow marine	0–40	Hendricks and Stevenson (2003), Timmons et al. (2012)
Solomon Temple		280	Ssss	Fluvial	0	Hendricks and Stevenson (2003)
Camanshe Point		130–188	Ssss	Tidal flat, evaporitic	0	Hendricks and Stevenson (2003)
Ochoa	–1100	53–92	Ssss	Tidal flat, evaporitic	0	Hendricks and Stevenson (2003)
Cardenas Basalt	1100	240–300	BBBB	Marine/brackish eruption	0–40	Weil et al. (2003), Hendricks and Stevenson (2003), Timmons et al. (2005)
Nankoweap	782–	113	SSSs	Shallow marine/lacustrine	0–40	Ford and Dehler (2003), Dehler et al. (2017)
<u>Chuar Group</u>						
Tanner		156–195	Dsss	Shallow marine, sub-/inter-tidal	20–60	Ford and Dehler (2003)
Jupiter		265–462	ssss	Shallow marine, tidal flat	0–40	Ford and Dehler (2003)
Carbon Canyon	–758	350–890	DDDs	Shallow marine, tidal flat	0–40	Ford and Dehler (2003), Rooney et al. (2018)
Duppa	755–	104–625	ssss	Shallow marine, tidal flat	0–40	Ford and Dehler (2003)
Carbon Butte	–751	62–120	SSss	Shallow marine, tidal flat	0–40	Ford and Dehler (2003), Rooney et al. (2018)
Awatubti	751–	171–300	ssss	Shallow marine, sub-tidal to shoreline	0–60	Ford and Dehler (2003), Rooney et al. (2018)
Walcott	–729	231–281	DDDs	Shallow marine, sub-tidal	0–60	Ford and Dehler (2003), Rooney et al. (2018)
Sixtymile	572–509	36–64	SSSs	Continental	0	Ford and Dehler (2003), Karlstrom et al. (2018)
<u>Tonto Group</u>						
Tapeats	509–505	30–120	SSSS	Fluvial, shallow marine	0–40	Middleton and Elliot (2003), Karlstrom et al. (2018)
Bright Angle Shale	505–501	82–137	SSss	Shallow marine, sub-tidal	40–80	Middleton and Elliot (2003), Karlstrom et al. (2018)
Muav Limestone	501–497	42–252	DDDs	Shallow marine, sub-tidal	20–60	Middleton and Elliot (2003), Karlstrom et al. (2018)
Temple Butte	391–380	0–220	DDDD	Shallow marine, sub-tidal	20–60	Beus (2003a)
Redwall Limestone	353–337	120–245	LLLD	Shallow marine, epeiric sea	20–60	Beus (2003b), Table 1
Surprise Canyon	327–325	0–122	SLss	Continental, shallow marine	0–40	Beus (2003b), Table 1
<u>Supai Group</u>						
Watahomigi	323–318	30–90	DLss	Shallow marine, shoreline	0–40	Blakey (2003), Table 1
Manakacha	318–311	45–90	SSSs	Aeolian	0	McKee (1975), McKee (1982), Blakey and Knepp (1989), Blakey (2003)
Wescogame	303–299	30–60	SSSL	Aeolian	0	McKee (1975), McKee (1982), Blakey and Knepp (1989), Blakey (2003)
Esplanade	299–282	60–240	SSSS	Shallow marine, aeolian	0–40	McKee (1975), McKee (1982), Blakey and Knepp (1989), Blakey (2003)
Hermit Coconino Sandstone	282–	30–270	ssss	Fluvial	0	Blakey and Knepp (1989), Blakey (2003)
Toroweap		20–183	SSSS	Aeolian	0	Middleton et al. (2003)
Kaibab	–269	75–168	SSLX	Shallow marine, tidal	0–40	McColloch et al. (1994), Turner (2003)
Moenkopi	250–245	90–120	DLSS	Shallow marine, tidal	0–40	Hopkins and Thompson (2003)
		0–122	Lsss	Shallow marine, continental	0–60	Hintze (1988), Woods (2009), Hautmann et al. (2013)

*B—Basalt, D—Dolostone, L—Limestone, S—Sandstone, s—Shale, X—Salt. Four-letter codes indicate relative proportions of each lithology.

†Based on sedimentary facies described in the quoted references.

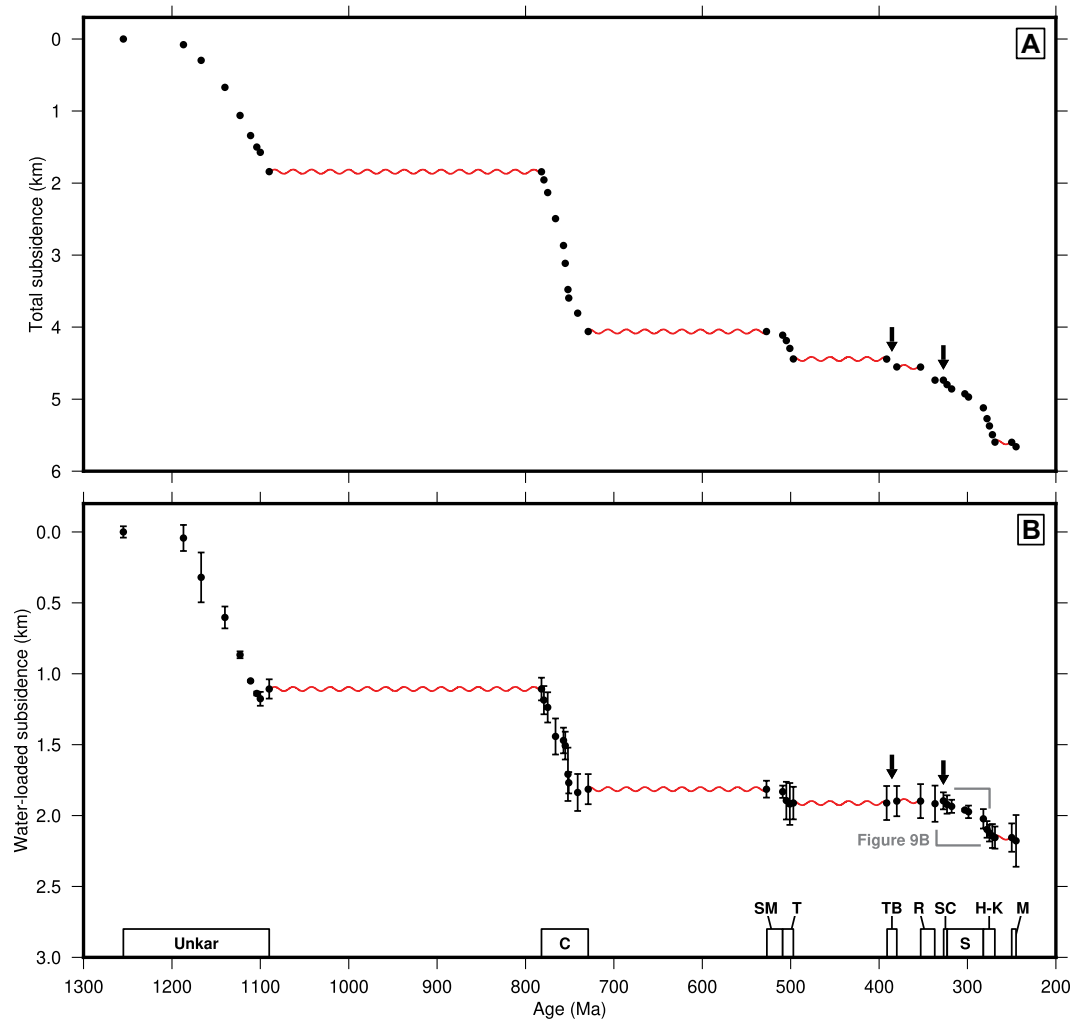


Figure 8. Subsidence curve for Grand Canyon region is shown. (A) Plot of observed subsidence as a function of time is based upon stratigraphic logs of Hintze (1988) and Beus and Morales (2003). Black circles—uncorrected subsidence measurements determined from average stratigraphic thicknesses; red wiggly lines—loci of major erosional unconformities; black arrows—timings of transient landscapes. (B) Plot of backstripped and water-loaded subsidence measurements as a function of time. Black circles with vertical error bars—water-loaded estimates that include stratal thickness uncertainties and paleobathymetric uncertainties. Major stratigraphic groups are labeled along base (C—Chuar Group; SM—Sixty-Mile Formation; T—Tonto Group; TB—Temple Butte Formation; R—Redwall Limestone; SC—Surprise Canyon Formation; S—Supai Group; H-K—Hermit-Kaibab Formations; M—Moenkopi Formation). Gray box highlights transient subsidence event shown in Figure 9B.

characterized by normal faulting and basaltic magmatism, which suggests that lithospheric thinning also took place (Timmons et al., 2001). No subsidence is recorded for a period of ~300 m.y., following which the Neoproterozoic Chuar Group was deposited (780–730 Ma). During this time, the rate of tectonic subsidence was approximately constant. Growth normal faulting is consistent with deposition within a rift setting associated with the break-up of Rodinia (Karlstrom et al., 2000; Timmons et al., 2001; Dehler et al., 2017; Rooney et al., 2018). A ~200 m.y. gap in the record precedes Cambrian deposition of the recently reclassified Sixtymile Formation (ca. 530–510 Ma; Karlstrom et al., 2018) and the Tonto Group (ca. 510–500 Ma; Rose, 2006; Karlstrom et al., 2018). This smaller episode of tectonic subsidence may represent the final stages of rifting within southern Rodinia (Karlstrom et al., 2018). A third stratigraphic gap spanning Ordovician and Silurian times follows deposition of the Tonto Group. The Temple Butte Formation was deposited in thin channels that are incised into the top of the Tonto Group.

Subsequently, the Redwall Limestone was deposited in a shelfal setting (Rose, 1976; Poole and Sandberg, 1977; Gutschick and Sandberg, 1983; Beus and Morales, 2003). Neither of these units records significant tectonic subsidence.

The incised upper surface of the Redwall Limestone and the lower unit of the Surprise Canyon Formation indirectly record regional uplift (i.e., negative subsidence), which is represented in subsidence-time space by a horizontal unconformity that lasts ~10 m.y. Marine fauna from the middle and upper units demonstrate that regional subsidence recommences and continues with a minor break into the overlying Supai Group. In the Grand Canyon region, this paired excursion of uplift and subsidence is not structurally controlled but represents a relative base-level fall and subsequent recovery (McKee, 1982; Beus and Morales, 2003). Explanations for this paired excursion must account for two significant observations. First, regional uplift has an amplitude of at least 280 ± 90 m and develops over a period of ~10 m.y. Secondly, regional subsidence commences at ca. 325 Ma and appears

to decrease exponentially by ~130 m over the following 50 m.y. There are three possible explanations for these linked observations: glacio-eustasy, flexure, and decay of a thermal anomaly. Waxing and waning of ice sheets is a recognized mechanism for producing relative sea-level fall and rise that is often invoked to explain Carboniferous stratigraphic observations. As we have discussed, there are two difficulties in invoking this mechanism to account for the Surprise Canyon Formation base-level changes. First, the required sea-level fall would have to have a minimum amplitude of ~200 m, which is considerably greater than the maximum amplitude that is expected to be generated by Carboniferous glacio-eustasy. Secondly, recovery by subsidence appears to take place over tens of millions of years, which is also inconsistent with glacio-eustasy.

Patterns of water-loaded subsidence across western North America during Carboniferous times are often attributed to flexural bending by mountain ranges associated with the Antler orogeny and the Ancestral Rocky Mountains (Fig. 7B; Giles and Dickinson, 1995; Barbeau,

2003; Sturmer et al., 2018). The extent to which flexural loading of the lithosphere can account for the post-Redwall subsidence excursion observed in the Grand Canyon region depends on the proximity of potential loads and upon the effective elastic thickness, T_e . By matching sediment thickness patterns, Barbeau (2003) estimated T_e to be ~ 25 km in the Paradox basin, which is bounded by the Uncompahgre Uplift located northeast of the Grand Canyon region (Fig. 7B). This analysis enables the wavelength over which lithospheric loading can produce vertical displacement to be gauged. The distance from a given load to the crest of the forebulge, x_b , is given by:

$$x_b = \pi \left[\frac{4ET_e^3}{12g(1-v^2)(\rho_m - \rho_w)} \right]^{\frac{1}{4}}, \quad (1)$$

where $E = 10^{11}$ kg m $^{-1}$ s $^{-2}$ is Young's modulus, $g = 9.81$ m s $^{-2}$ is gravitational acceleration, $v = 0.25$ is Poisson's ratio, and $\rho_m = 3.2$ Mg m $^{-3}$ and $\rho_w = 1.03$ Mg m $^{-3}$ are the densities of mantle and sea water, respectively (e.g., Gunn, 1943; Watts, 2001). If $T_e = 25$ km, $x_b = \sim 225$ km, which implies that only loads that are located within ~ 200 km of the Grand Canyon region are capable of generating significant subsidence. This inference is consistent with the interpretation of Giles and Dickinson (1995), who identified forebulge unconformities across eastern Nevada and western Utah within ~ 150 km of the Antler range front. The present-day expressions of the Uncompahgre Uplift and the remnant Antler orogen lie 300–500 km east and west of the Grand Canyon region, respectively. The more modest Zuni-Defiance Uplift is located 200–400 km to the southeast (Fig. 7). Estimates of the amount of post-Carboniferous rifting across the Basin and Range Province vary significantly but stretching factors could be as large as two (e.g., Zoback et al., 1981). If so, considerable portions of the Grand Canyon region were still probably >200 km distant from the Antler orogen. On this basis, we suggest that the post-Redwall subsidence excursion is unlikely to have been generated by flexural loading. Furthermore, flexural subsidence is generally convex upward, and the observed excursion is not.

Thermal Model

Here, we propose an alternative mechanism for generating transient uplift and subsidence. This mechanism is inspired by observational studies of transient buried landscapes discovered in outcrop and on three-dimensional seismic reflection surveys along continental margins that fringe the Icelandic plume in the North Atlantic

region (Dam, 2002; Hartley et al., 2011; Stucky de Quay et al., 2017). These Paleogene terrestrial landscapes are sandwiched between marine sedimentary deposits and are generated by transient uplift episodes with amplitudes on the order of 100 m that cannot be explained by glacio-eustasy. Instead, they appear to have been generated by thermal anomalies that horizontally advect through an asthenospheric channel away from the conduit of the Icelandic plume. This convective mechanism is corroborated by Neogene V-shaped ridge activity recorded in the oceanic basins on either side of the present-day Icelandic plume (Parnell-Turner et al., 2014). Globally, it is becoming clear that asthenospheric thermal anomalies can play a significant role in generating regional epeirogenic uplift and magmatism (e.g., India, Anatolia, and Africa; Richards et al., 2016; McNab et al., 2018; Ball et al., 2019; Stephenson et al., 2021). In these locations, emplacement of anomalously hot material within an asthenospheric channel appears to coincide with significant and rapid thinning of the lithospheric mantle. Beneath the lithosphere, surface-wave tomographic models show that slow shear-wave velocity anomalies occur within a layer that is 150 ± 50 km thick (e.g., Priestley and McKenzie, 2013; Schaeffer and Lebedev, 2013). By calibrating these tomographic models with an oceanic plate cooling model, asthenospheric temperature anomalies of 50–100 °C have been obtained (Richards et al., 2020).

We can explore the possibility that the transient landscape recorded by the Surprise Canyon Formation was generated by dynamic topography associated with a sub-lithospheric thermal anomaly using a simple analytical model. The principal question is whether a thermal anomaly can account for both the amplitude of base-level fall recorded by Surprise Canyon Formation paleochannels and the timescale of ensuing subsidence. Exactly what constitutes dynamic topography is often debated in the literature. Here, we employ the widely accepted definition first described by Hager and Richards (1989), although we are aware that other definitions are sometimes used. Deflections of the Earth's surface are driven by viscous stresses that are generated by density contrasts within the convecting mantle. These deflections represent dynamic topography and are given by:

$$\delta a^{lm} = \frac{1}{\Delta \rho_a} \int_r^a A^l(r) \delta \rho^{lm}(r) dr, \quad (2)$$

where $\delta \rho^{lm}$ is dynamic topography of the Earth's surface and $A^l(r)$ are the normalized surface response kernels as a function of radius, r , for a putative density anomaly located at different depths

within the mantle. a is the Earth's radius, $\Delta \rho_a$ is the density contrast at the surface boundary, and $\delta \rho^{lm}(r)$ represents mantle density anomalies. Superscripts l and m refer to spherical harmonic degree and order, respectively. The value of $A^l(r)$ depends upon the radial viscosity structure of the mantle. It is important to appreciate that $A \rightarrow 1$ within the uppermost mantle close to the base of the lithospheric plate for all values of l regardless of viscosity structure, which means that $\delta a \rightarrow \delta \rho / \Delta \rho_a$ (Hager and Richards, 1989; Colli et al., 2016). Consequently, the sum of the flow and isostatic components of dynamic topography within, say, an asthenospheric channel immediately beneath the lithospheric plate can be confidently approximated using a thermal isostatic relationship (Richards et al., 2020; Stephenson et al., 2021).

In our model, we assume that a layer of hot asthenosphere is emplaced within a channel beneath continental lithosphere that has a crustal thickness of t_c and a lithospheric thickness of a (Fig. 9A). The initial thermal structure of the lithosphere is calculated by assuming a constant internal heat production of $H = 1.07 \times 10^{-6}$ W m $^{-3}$ within the crust and sub-plate isentropic gradient that is consistent with a mantle potential temperature, $T_p = 1330$ °C. Emplacement of the thermal anomaly is assumed to be instantaneous, which is in accord with the rapid asthenospheric velocities recorded by V-shaped ridge activity associated with the Icelandic plume (Hartley et al., 2011; Parnell-Turner et al., 2014). For simplicity, we ignore the possibility that continental lithosphere may thin when a thermal anomaly is emplaced (Yuen and Fleitout, 1985; Davies, 1994; Ball et al., 2021).

Intrusion of a thermal anomaly that has a thickness of X and an excess temperature of ΔT generates regional uplift, which is given by:

$$U = \frac{X \Delta T}{1 - \alpha T_b}, \quad (3)$$

where $\alpha = 3.5 \times 10^{-5}$ °C $^{-1}$ is the thermal expansivity, $T_b = T_p + \phi(a + X)$ is the temperature at the base of the column, and $\phi = 4.5 \times 10^{-4}$ °C m $^{-1}$ is the isentropic gradient (Rudge et al., 2008). Note that this expression assumes that the calculated topography is air loaded. Fluvial erosion will isostatically amplify regional uplift, and the maximum amount of regional denudation, D , is given by:

$$D = \frac{U(\rho_o(1 - \alpha T_b))}{\rho_o(1 - \alpha T_b) - \rho_d}, \quad (4)$$

where $\rho_o = 3.3$ Mg m $^{-3}$ is a reference mantle density and ρ_d is the density of denuded material. In the case of the Surprise Canyon Formation, preservation of a fluvially eroded landscape

indicates that regional uplift was not completely amplified into the maximum amount of denudation (i.e., there is partial denudation).

Following rapid uplift and denudation, the thermal anomaly decays as a function of time and generates regional subsidence (Fig. 9C; Appendix 1). In the absence of denudation, this subsidence pulse decays away exponentially, and the total additional subsidence equals U (Fig. 9C; Appendix 1). If partial denudation occurs, initial uplift is amplified, and additional accommodation space is created that can be filled during subsequent subsidence. In both cases, cooling of the thermal anomaly determines how subsidence varies as a function of time. The temperature history of the thermal anomaly is calculated by solving the one-dimensional heat equation using standard Fourier series expansion (Appendix 1).

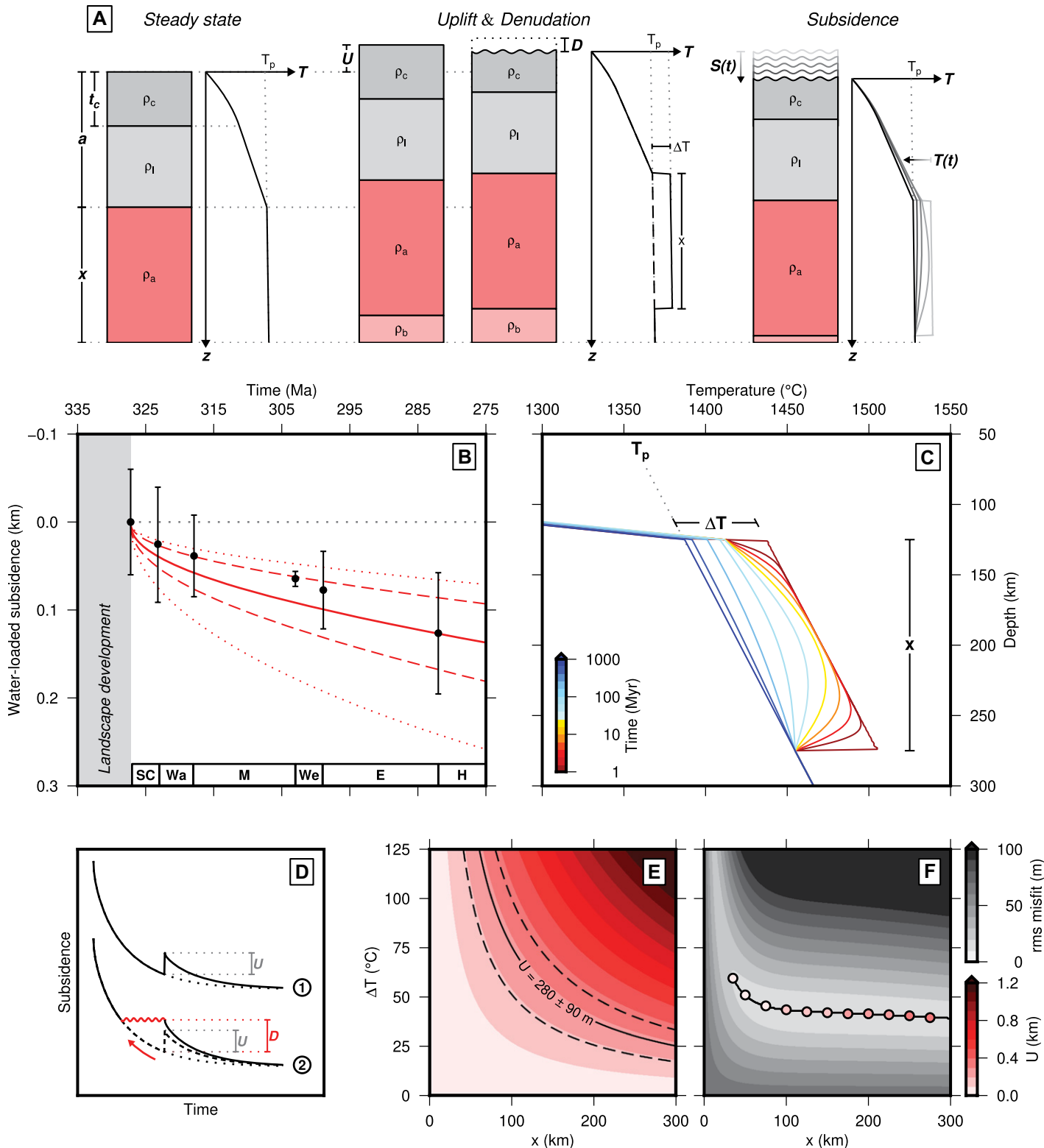


Figure 9. Thermal subsidence analysis is shown. (A) Schematic cartoon outlines subsidence modeling procedure (not to scale; see main text for explanation and for definition of all symbols). Dark gray/light gray rectangles—crust/lithospheric mantle; red rectangle—asthenosphere; rectangle with wavy pattern—sedimentary deposition. Columns are paired with three plots of temperature as a function of depth that show: (i) initial temperature structure; (ii) perturbed temperature structure; and (iii) temporally evolving temperature structure. T_p —potential temperature of underlying asthenospheric mantle; ΔT and X —size and thickness of asthenospheric temperature anomaly; $T(t)$ —temperature as function of time. (B) Observed and calculated subsidence as a function of time relative to base Surprise Canyon Formation. Black circles with vertical error bars—water-loaded subsidence measurements from Grand Canyon region that include stratal thickness uncertainties and paleobathymetric uncertainties (see Fig. 8). Vertical gray band—period of time during which fluvial landscape develops; solid red line—calculated subsidence curve that assumes that $\Delta T = 50^\circ\text{C}$, $X = 150\text{ km}$ for regional uplift of 280 m; pair of dashed red lines—subsidence curves for extremal regional uplifts of 190 m and 370 m; pair of dotted red lines—subsidence curves for extremal channel thicknesses of 100 km and 200 km; gray dotted line—reference level; labeled strip along base—stratigraphic template (SC—Surprise Canyon Formation, Wa—Watahomigi Formation, M—Manakacha Formation, We—Wescogame Formation, E—Esplanade Formation, H—Hermit Formation). (C) Evolution of temperature as a function of depth for best-fitting thermal model. Gray dotted line—isentropic temperature profile; T_p —potential temperature of asthenospheric mantle; ΔT and X —size and thickness of asthenospheric temperature anomaly; suite of colored lines—calculated temperature history, $T(z,t)$, in accordance with color bar. (D) Sketches of expected subsidence as a function of time showing (1) uplift-subsidence transient excursion and (2) consequent denudation-subsidence excursion. U —amplitude of regional uplift; D —amplitude of consequent regional denudation; black dotted curves—expected subsidence trajectories in absence of any transient event; red wiggly horizontal line—regional unconformity; red arrow—extent of removal of existing subsidence record by denudation event. Dashed black line of (2) represents solid line of (2). (E) Temperature anomaly, ΔT , is plotted as a function of thickness of anomaly, X . Red contour lines—amplitude of regional uplift, U , calculated for combinations of values of ΔT and X contoured in accordance with color bar on right-hand side. Labeled solid/dashed black lines—trade-off relationship between ΔT and X for which $U = 280 \pm 90\text{ m}$. (F) Residual misfit between observed and calculated subsidence curves as a function of X and ΔT is contoured in accordance with gray scale bar on right-hand side. Colored circles—values of regional uplift along global minimum in accordance with color bar on right-hand side.

In the case of maximum denudation, the water-loaded subsidence history, S , is given by:

$$S(t) = \frac{\rho_w \alpha (a + X)}{\rho_w (1 - \alpha T_b) - \rho_w} \\ \sum_{m=0}^{\infty} \frac{2A_n}{n\pi} \exp\left(-\frac{n^2 t}{\tau}\right), \text{ with } n = 2m + 1, \quad (5)$$

where $\rho_w = 1.03\text{ Mg m}^{-3}$ is the density of sea water, τ is a thermal time constant, and A_n are coefficients determined by the initial condition (Appendix 1). In this way, transient uplift subsidence histories can be calculated for a range of values of X and ΔT .

We now compare observed and calculated subsidence histories of the Grand Canyon region (Fig. 9C). Since there is no direct evidence for significant post-Carboniferous crustal thickening or thinning in the Grand Canyon region, we assume that $t_c = 40\text{ km}$, based upon present-day receiver function estimates (Shen and Ritzwoller, 2016). Note that our calculations are not especially sensitive to this value. Lithospheric thickness is assumed to be $a = 125\text{ km}$, which is the approximate steady-state thickness of Phanerozoic continental lithosphere (e.g., Parsons and Sclater, 1977; Parsons and McKenzie, 1978; Richards et al., 2018). Instantaneous emplacement of the asthenospheric thermal anomaly and subsequent denudation are assumed to occur at a time that corresponds to the base of the Surprise Canyon Formation (i.e., ca. 327 Ma). Observed and calculated subsidence histories are then compared over a period of time that lasts from the

Surprise Canyon Formation until the Hermit Formation that lies approximately halfway through the Supai Group. We assume that this duration represents the time over which the thermal anomaly decays. If the asthenospheric channel is assumed to be $150 \pm 50\text{ km}$ thick, an anomaly of $\sim 65 \pm 35^\circ\text{C}$ is required to generate $280 \pm 90\text{ m}$ of air-loaded regional uplift (Fig. 9E). Cooling of such an anomaly can explain the magnitude and rate of subsidence following incision of the Redwall Limestone (Fig. 9C). To minimize the misfit between observed and calculated subsidence values, we next carried out a two-parameter sweep through X - ΔT space (Figs. 9E–9F). The trial misfit function is given by:

$$\chi^2 = \sqrt{\frac{1}{N} \sum_{i=1}^N \frac{(S_i^o - S_i^c)^2}{\sigma_i^2}}. \quad (6)$$

N is the number of observations. The superscripts o and s represent observed and calculated subsidence values where σ is the uncertainty. It is important to emphasize that significant trade-offs exist in these calculations. Figure 9E demonstrates that regional uplift values of $U = 280 \pm 90\text{ m}$ can be generated by many different combinations of X and ΔT since these parameters trade off negatively against each other. To minimize the misfit between observed and calculated subsidence values, the value of ΔT is required to be $40 \pm 10^\circ\text{C}$, but the value of X is less well constrained (Fig. 9F).

We conclude that the transient uplift subsidence history recorded by the stratigraphic record

that straddles the Surprise Canyon Formation can be satisfactorily matched by invoking a subplate thermal anomaly that subsequently decays over time. A more complex model that includes thinning of the lithospheric mantle fits the observations equally well. For example, lithospheric mantle thinning of 30–40 km and replacement by asthenospheric material with potential temperatures of up to a few tens of degrees above that of ambient mantle yields a satisfactory fit, which is consistent with analysis of regions experiencing present-day epeirogenic uplift (e.g., Klöcking et al., 2018; Ball et al., 2019).

Throughout these calculations, we have assumed that all of the subsidence following incision of the Redwall Limestone is generated by cooling of an asthenospheric anomaly. However, it is possible that the region was undergoing background subsidence following, for example, a phase of Cambrian rifting (e.g., Bond et al., 1983; Bond et al., 1985; Levy and Christie-Blick, 1991; Dickinson, 2004; Karlstrom et al., 2018). In this case, smaller anomalies are required to fit observed subsidence. We also made the simplifying assumption that thermal anomalies cool only by conduction. At asthenospheric depths, anomalies may also be expected to lose heat by advection. For example, they may spread and thin as viscous gravity currents (e.g., Bercovici and Lin, 1996). If such advective processes contribute significantly to cooling, subsidence would occur more rapidly than we predict. We note in passing that transient uplift and subsidence can also be generated by applying and removing viscous stresses at the base of the plate (Flament

et al., 2013). This process has been invoked to explain Cenozoic uplift of the Colorado Plateau and the presence of a prominent Neogene unconformity in the adjacent Rio Grande rift (van Wijk et al., 2010, 2018; Karlstrom et al., 2012). It is conceivable that varying patterns of viscous stresses could account for vertical motions on the order of hundreds of meters at timescales of several million years.

DISCUSSION

The Surprise Canyon Formation represents a period of transient base-level fall during which marine carbonates of the Redwall Limestone were exposed, incised, and then resubmerged. Allowing for the effects of compaction, base-level fall of at least 200 m is required. Exposure and incision occurred over a <10 m.y. period in early Serpukhovian times (Fig. 6). The magnitude and timing of this base-level fall are inconsistent with current reconstructions of Carboniferous glaciation, in which total sea-level change is thought to be restricted to ~50 m and ice-sheet extent, and therefore sea-level lowstand, peak in latest Serpukhovian and earliest Bashkirian times (e.g., Horton et al., 2010, 2012; Montañez and Poulsen, 2013). Detrital zircon records also suggest that a coincident and transient reorganization of regional networks occurred, consistent with a phase of long wavelength regional uplift (Fig. 5; Gehrels et al., 2011). Thus, the stratigraphic relationships described here appear to be best explained by a phase of transient uplift. Despite evidence for significant crustal shortening in nearby ranges of the Ancestral Rocky Mountains, there is no evidence for such deformation in the Grand Canyon region during Carboniferous times (e.g., Kluth and Coney, 1981; Dickinson and Lawton, 2003; Leary et al., 2017). Furthermore, crustal deformation would be unable to account for the transient nature of uplift represented by the Surprise Canyon Formation. It also appears that, given local estimates of the lithosphere's elastic thickness and the distance to known Ancestral Rocky Mountain range fronts, flexural loading of the lithosphere cannot explain uplift and subsequent subsidence of the Grand Canyon region (Fig. 7; Barbeau, 2003).

A more plausible mechanism for generating transient uplift and subsidence of the required magnitude may be emplacement and decay of an asthenospheric temperature anomaly. This process has been invoked to explain the generation of Paleogene transient landscapes that are now buried in the Faroe-Shetland and North Sea sedimentary basins. These landscapes are recorded on calibrated three-dimensional seismic reflection surveys (Shaw Champion et al., 2008; Hartley et al., 2011; Stucky de Quay et al., 2017). In

these examples, uplift and subsidence of up to ~800 m occurred over a period of a few million years. Hartley et al. (2011) proposed that the rapid phases of uplift and subsidence observed are best explained by lateral advection of hot pulses of asthenospheric mantle away from the center of the Icelandic plume.

Uplift and subsidence recorded by the Surprise Canyon Formation and overlying units are considerably slower than observed in Paleogene times around the Icelandic plume. In the Grand Canyon region, uplift and incision occur within ~10 m.y., and subsequent subsidence apparently continues for at least ~50 m.y. Furthermore, there were no known mantle plumes in the vicinity of the Grand Canyon region during Carboniferous times. However, it is becoming clear that thermal anomalies capable of supporting hundreds of meters of topography are a pervasive feature of the upper mantle at the present day. Global analyses of oceanic residual depth anomalies (i.e., depths relative to global age-depth relationships and corrected for crustal thickness variations) reveal a complex planform of convective support with amplitudes of $\sim\pm 1$ km and wavelengths of $\sim 10^3$ km (Menard, 1973; Cochran and Talwani, 1977; Cazenave et al., 1986, 1988; Hoggard et al., 2016, 2017). It is likely that this planform reflects a combination of topographic support from flow and temperature variations within the convecting mantle and from thickness and density variations in the lithospheric mantle (e.g., Phipps Morgan et al., 1995; Flament et al., 2013; Davies et al., 2019). By calibrating seismic tomographic models, Richards et al. (2020) show that the bulk of this signal can be explained by temperature variations of ± 50 – 100 °C on length scales of 10^3 km within a 150 ± 50 -km-thick asthenospheric channel beneath the base of the plate. The presence of a low-viscosity channel within which asthenospheric anomalies can circulate, independent of plate motions, is consistent with measurements of seismic anisotropy from the Pacific Ocean (Lin et al., 2016).

On the continents, Cenozoic growth of domes and plateaux has also been attributed to the presence of hot asthenospheric material located immediately beneath the plate. In many cases, these features are linked with intraplate magmatism and thinning of the lithospheric mantle (e.g., Burke, 1996; Wilson and Downes, 2006; Ball et al., 2021). Similar processes have been invoked to explain large-scale Cenozoic uplift of western North America (Bird, 1979; Fitton et al., 1991; van Wijk et al., 2010; Karlstrom et al., 2012; Roberts et al., 2012; Klöcking et al., 2018).

Several lines of evidence imply that a convective process of the kind described above could

have generated transient uplift, denudation, and subsidence recorded by the Surprise Canyon Formation and subsequent units. Such processes can generate vertical motions of appropriate amplitudes, are not associated with significant crustal deformation, and appear to be relatively ubiquitous at least throughout Cenozoic times. The localized occurrence of a heavy mineral assemblage, including pristine olivine, pyroxene, and hornblende grains in one Surprise Canyon Formation paleovalley, suggests that there was a local source of mafic magmatic material (Grover, 1989, p. 170–173). Magnitudes and timescales of the regional uplift subsidence event can be explained by the emplacement and subsequent cooling of a thermal anomaly immediately below the lithospheric plate (Fig. 9). Best-fitting models require temperature anomalies of 40 ± 10 °C, which fall within the range of values obtained from tomographic models and basaltic geochemistry in modern examples of regional epeirogeny (e.g., McNab et al., 2018; Klöcking et al., 2018; Ball et al., 2019, 2021). We note that viscous stresses imposed on the base of the plate by different forms of mantle flow may operate on similar timescales and length scales. If we include the approximately contemporaneous exposure and incision on the Leadville and Madison Shelves, the affected length of passive margin was at least ~ 1500 km, which again is consistent with equivalent features observed in the present day (De Voto, 1988; Sando, 1988; Hoggard et al., 2016, 2017). If age estimates for these sequences are accurate, base-level fall and incision appears to have affected the more northern Madison Shelf a few million years earlier than the Redwall Shelf of the Grand Canyon region (Fig. 6). This apparent southward migration cannot easily be accounted for by global sea-level variation, but it is consistent with horizontal advection of an asthenospheric thermal anomaly beneath the plate, translation of the plate over a stationary anomaly, or some combination of the two. Paleozoic plate reconstructions do suggest that the North American plate was drifting northeastward during middle Carboniferous times (e.g., Matthews et al., 2016).

Current efforts to reconstruct convective topographic support through geologic time heavily rely upon numerical modeling. One approach involves estimating mantle density structure through time based on histories of plate motion and subduction (e.g., Ricard et al., 1993; Flament et al., 2013). Alternatively, estimates of present-day density structure derived from seismic tomographic models can be used in backward advection calculations or iterative adjoint procedures (e.g., Bunge et al., 2003; Conrad and Gurnis, 2003; Spasojevic et al., 2009). There is a paucity of observational constraints with which

to test the predictions of these models and our understanding of mantle convection in the geologic past. Here, we have demonstrated that quantitative information about the growth and decay of transient uplift events can be obtained through careful analysis of buried ancient landscapes. With relict landscapes identified throughout the North Atlantic region, this example highlights the potential of these phenomena to provide powerful constraints on mantle convective processes as a function of geologic time (Hartley et al., 2011; Stucky de Quay et al., 2017).

CONCLUSIONS

The Surprise Canyon Formation of the Grand Canyon region represents a dramatic period of transient base-level fall during Carboniferous times. It is underlain by carbonates of the Redwall Limestone, which form part of an extensive shelf system that covered much of western North America in Mississippian times. Over a period of <10 m.y., base-level fall of at least 200 m resulted in exposure, karstification, and incision of this carbonate platform. Subsequent base-level rise triggered renewed deposition in initially terrestrial and then later marine environments. A prolonged period of subsidence followed that was apparently not related to regional rifting or flexural effects of the Ancestral Rocky Mountains. The timing and magnitude of required base-level fall makes eustatic sea-level change an unlikely cause. Instead, a regional transient uplift event is more plausible. Such an event could be driven by the arrival of hot asthenospheric material, a process that is linked to epeirogenic uplift in various locations at the present day. Plausible anomalous asthenospheric temperatures are able to reproduce the magnitude of initial uplift and the magnitude and timescale of subsequent subsidence. The apparent occurrence of contemporaneous mafic magmatism, and the possible migration of uplift and landscape development from north to south, are both consistent with this conceptual model. Detrital zircon geochronologies also imply that transient uplift may have caused the reorganization of regional drainage networks, resulting in an arrangement which, at least in part, persisted for the remainder of Paleozoic times (Gehrels et al., 2011). These results add to a growing body of evidence that suggests that ancient transient landscapes can record important information about convective processes throughout geologic time.

APPENDIX 1. THERMAL MODEL

The one-dimensional heat equation that describes the evolution of temperature, T , as a function of time, t , and depth, z , can be written as:

$$\rho c_p \frac{\partial T}{\partial t} = k \frac{\partial^2 T}{\partial z^2} + H, \quad (\text{A1})$$

where ρ is density, c_p is specific heat capacity, k is thermal conductivity, and H is internal heat production. All notation and parameter values used are summarized in Table A1. We approximate the thermal structure of the crust and upper mantle using a simple three-layer model: a crustal layer of thickness t_c with internal heat production, a lithospheric mantle layer of thickness $a - t_c$, and an asthenospheric channel of thickness X . Heat production is assumed to be negligible within the mantle layers. We first obtain the steady-state temperature structure, $T_s(z)$. The temperature structure is assumed to obey Equation (A1) within the lithosphere and lie on the mantle isentrope within the asthenosphere. Imposing boundary conditions such that the temperature at the surface is zero and temperature and heat flow are continuous between each layer leads to:

$$T_s(z) = \begin{cases} \left[\frac{T_a}{a} + \frac{Ht_c}{k_c} \left(1 - \frac{t_c}{2a} \right) \right] z - \frac{H}{2k_c} z^2, & \text{for } 0 \leq z \leq t_c, \\ \left[\frac{T_a}{a} - \frac{Ht_c^2}{2k_c a} \right] (z - a) + T_a, & \text{for } t_c \leq z \leq a, \\ T_p + \phi z, & \text{for } z \geq a, \end{cases} \quad (\text{A2})$$

where T_p is the mantle potential temperature, ϕ is the isentropic gradient, $T_a = T_p + \phi a$ is the temperature at the base of the lithosphere, and k_c is the thermal conductivity within the crust. Values of H were chosen so that the surface heat flux is equal to 63 mW m⁻², an approximate average value for Phanerozoic continental lithosphere (Lucazeau, 2019). To investigate the response of the temperature structure to perturbation, we solve Equation (A1) using Fourier series (Carslaw and Jaeger, 1959). This approach assumes that all cooling within the lithosphere and asthenosphere occurs by conduction. A general solution takes the form:

$$T(z,t) = T_s + \sum_{n=1}^{\infty} A_n \sin\left(\frac{n\pi z}{a+X}\right) \exp\left(-\frac{n^2 t}{\tau}\right). \quad (\text{A3})$$

τ is the thermal time constant, which is given by:

$$\tau = \frac{(a+X)^2}{\pi^2 \kappa}, \quad (\text{A4})$$

where $\kappa = k/\rho c_p$ is the thermal diffusivity. Average values of k , ρ , and c_p for the crust and mantle are used to compute κ . A_n are coefficients given by:

$$A_n = \frac{2}{a+X} \int_0^{a+X} (T_o - T_s) \sin\left(\frac{n\pi z}{a+X}\right) dz, \quad (\text{A5}),$$

where T_o is the initial condition. We assume instantaneous arrival of a temperature anomaly, ΔT , in the asthenospheric channel, so that:

$$T_o = \begin{cases} T_s, & \text{for } 0 \leq z \leq a, \\ T_p + \Delta T + \phi z, & \text{for } a \leq z \leq a+X, \end{cases} \quad (\text{A6})$$

The expression for A_n becomes:

$$A_n = \frac{2}{a+X} \int_a^{a+X} \Delta T \sin\left(\frac{n\pi z}{a+X}\right) dz, \quad (\text{A7})$$

$$= \frac{2\Delta T}{n\pi} \left[\cos\left(\frac{n\pi a}{a+X}\right) + (-1)^n \right],$$

Water-loaded subsidence associated with this thermal anomaly, S , can be calculated using a simple isostatic balance and by integrating Equation (A3) over the depth of the column to obtain average temperature anomalies as a function of time. Hence,

$$S(t) = \frac{\rho_o \alpha (a+X)}{\rho_o (1 - \alpha T_b) - \rho_w}$$

$$\left[\frac{1}{a+X} \int_0^{a+X} (T(t) - T_s) dz \right], \quad (\text{A8})$$

$$= \frac{\rho_o \alpha (a+X)}{\rho_o (1 - \alpha T_b) - \rho_w}$$

$$\sum_{n=1}^{\infty} \frac{A_n}{n\pi} \left(-\frac{n^2 t}{\tau} \right) [1 - \cos(n\pi)].$$

TABLE A1. NOTATION AND PARAMETER VALUES USED IN THERMAL CALCULATIONS

Symbol	Parameter	Value	Units
a	Lithospheric thickness	125×10^3	m
α	Thermal expansivity	3.5×10^{-5}	°C ⁻¹
c_p	Specific heat capacity	1080	J K kg ⁻¹
H	Crustal heat production	1.07×10^{-6}	W m ⁻³
k	Thermal conductivity	3.5	W m ⁻¹ K ⁻¹
k_c	Crustal thermal conductivity	2.5	W m ⁻¹ K ⁻¹
κ	Thermal diffusivity	$k/(\rho c_p) = 6.3 \times 10^{-6}$	m ² s ⁻¹
S	Water-loaded subsidence		m
ρ_o	Reference mantle density	3300	kg m ⁻³
ρ_w	Sea-water density	1030	kg m ⁻³
t	Time		s
t_c	Crustal thickness	40×10^3	m
T	Temperature		°C
T_a	Temperature at base of lithosphere	$T_p + \phi a = 1385$	°C
T_b	Temperature at base of column	$T_p + \phi(a+X)$	°C
T_p	Mantle potential temperature	1330	°C
T_s	Steady-state temperature		°C
ΔT	Temperature anomaly		°C
τ	Thermal time constant	$(a+X)^2/\pi^2 \kappa$	s
ϕ	Isentropic gradient	4.5×10^{-4}	°C m ⁻¹
X	Asthenospheric channel thickness		m
z	Depth		m

$1 - \cos(n\pi)$ is equal to zero for even n and equal to two for odd n . Hence,

$$S(t) = \frac{\rho_o \alpha (a + X)}{\rho_o (1 - \alpha T_b) - \rho_w} \sum_{m=0}^{\infty} \frac{2A_m}{n\pi} \exp\left(-\frac{n^2 t}{\tau}\right), \quad (A9)$$

with $n = 2m + 1$,

where ρ_o is a reference mantle density at standard pressure and temperature, ρ_w is the density of sea water, α is the thermal expansivity, and $T_b = T_p + \phi(a + X)$ is the temperature at the base of the column. Note that since the majority of temperature variation is restricted to the lithospheric and asthenospheric mantle, we used a reference density for the entire column that corresponds to that of the mantle.

ACKNOWLEDGMENTS

This project is supported by Shell Research. We are grateful to W. Ranney for generously sharing his photograph of the Surprise Canyon Formation at Fern Glen with us. We thank P. Ball, R. Clark, I. Frame, M. Hoggard, S. Humbert, A. Jackson, L. Kennan, D. Lyness, C. O'Malley, L. Middleton, F. Richards, V. Rodríguez Tribaldos, D. Smit, S. Stephenson, and K. Warners for their help. Two anonymous reviewers are thanked for providing detailed and constructive comments. Figures were prepared using Generic Mapping Tools software (Wessel et al., 2019). This work is Cambridge Earth Sciences contribution esc. 6030.

REFERENCES CITED

- Ahern, J.P., and Fielding, C.R., 2019, Onset of the Late Paleozoic glacioeustatic signal: A stratigraphic record from the paleotropical, oil-shale bearing Big Snowy Trough of Central Montana, USA: *Journal of Sedimentary Research*, v. 89, p. 761–783, <https://doi.org/10.2110/jsr.2019.44>.
- Al-Hajri, Y., White, N., and Fishwick, S., 2009, Scales of transient convective support beneath Africa: *Geology*, v. 37, p. 883–886, <https://doi.org/10.1130/G25703A.1>.
- Anderson, J.L., and Morrison, J., 1992, The role of anorogenic granites in the Proterozoic crustal development of North America, in Condie, K.C., ed., *Proterozoic Crustal Evolution*: New York, USA, Elsevier, p. 263–299, [https://doi.org/10.1016/S0166-2635\(08\)70121-X](https://doi.org/10.1016/S0166-2635(08)70121-X).
- Archer, A.W., and Greb, S.F., 1995, An Amazon-scale drainage system in the early Pennsylvanian of central North America: *The Journal of Geology*, v. 103, p. 611–627, <https://doi.org/10.1086/629784>.
- Ball, P.W., White, N.J., Masoud, A., Nixon, S., Hoggard, M.J., MacLennan, J., Stuart, F.M., Oppenheimer, C., and Kröpelin, 2019, Quantifying asthenospheric and lithospheric controls on mafic magmatism across North Africa: *Geochemistry, Geophysics, Geosystems*, v. 20, p. 3520–3555, <https://doi.org/10.1029/2019GC008303>.
- Ball, P.W., White, N.J., MacLennan, J., and Stephenson, S.N., 2021, Global influence of mantle temperature and plate thickness on intraplate volcanism: *Nature Communications*, v. 12, no. 2045, <https://doi.org/10.1038/s41467-021-22323-9>.
- Barbeau, D.L., 2003, A flexural model for the Paradox Basin: Implications for the tectonics of the Ancestral Rocky Mountains: *Basin Research*, v. 15, p. 97–115, <https://doi.org/10.1046/j.1365-2117.2003.00194.x>.
- Bercovici, D., and Lin, J., 1996, A gravity current model of cooling mantle plume heads with temperature-dependent buoyancy and viscosity: *Journal of Geophysical Research: Solid Earth*, v. 101, no. B2, p. 3291–3309, <https://doi.org/10.1029/95JB03538>.
- Beus, S.S., 1999, Megafossil paleontology of the Surprise Canyon Formation, in Billingsley, G.H., and Beus, S.S., eds., *Geology of the Surprise Canyon Formation of the Grand Canyon, Arizona*: Northern Arizona Bulletin, v. 61, p. 69–96.
- Beus, S.S., 2003a, Temple Butte Formation, in Beus, S.S., and Morales, M., eds., *Grand Canyon Geology* (2nd edition): New York, USA, Oxford University Press, p. 107–114.
- Beus, S.S., 2003b, Redwall Limestone and Surprise Canyon Formation, in Beus, S.S., and Morales, M., eds., *Grand Canyon Geology* (2nd edition): New York, USA, Oxford University Press, p. 115–135.
- Beus, S.S., and Martin, H., 1999, Age and correlation, in Billingsley, G.H., and Beus, S.S., eds., *Geology of the Surprise Canyon Formation of the Grand Canyon, Arizona*: Northern Arizona Bulletin, v. 61, p. 117–120.
- Beus, S.S., and Morales, M., eds., 2003, *Grand Canyon Geology* (2nd edition): New York, USA, Oxford University Press, 448 p.
- Beuthin, J.D., 1994, A sub-Pennsylvanian paleovalley system in the Central Appalachian Basin and its implications for tectonic and eustatic controls on the origin of the regional Mississippian–Pennsylvanian unconformity, in Dennison, J.M., and Ettensohn, F.R., eds., *Tectonic and Eustatic Controls of Sedimentary Cycles*: Tulsa, Oklahoma, USA, SEPM (Society for Sedimentary Geology), p. 107–120, <https://doi.org/10.2110/csp.94.04.0107>.
- Billingsley, G.H., 1999, Paleovalleys of the Surprise Canyon Formation in Grand Canyon, in Billingsley, G.H., and Beus, S.S., eds., *Geology of the Surprise Canyon Formation of the Grand Canyon, Arizona*: Northern Arizona Bulletin, v. 61, p. 17–52.
- Billingsley, G.H., 2000, Geological map of the Grand Canyon 30' × 60' quadrangle, Mohave and Coconino Counties, northwestern Arizona: U.S. Geological Survey Geologic Investigations Series I-2688, scale 1:100,000.
- Billingsley, G.H., and Beus, S.S., 1984, The Surprise Canyon Formation—an upper Mississippian and lower Pennsylvanian(?) rock unit in the Grand Canyon, Arizona: U.S. Geological Survey Bulletin 1605-A, p. A27–A33.
- Billingsley, G.H., and Beus, S.S., eds., 1999, *Geology of the Surprise Canyon Formation of the Grand Canyon, Arizona*: Northern Arizona Bulletin, v. 61, 254 p.
- Billingsley, G.H., and McKee, E.D., 1982, Pre-Supai buried valleys, in *The Supai Group of the Grand Canyon*: U.S. Geological Survey Professional Paper 1173, p. 137–154.
- Billingsley, G.H., and Wellmeyer, J.L., 2003, Geological map of the Mount Trumbull 30' × 60' quadrangle, Mohave and Coconino Counties, northwestern Arizona: U.S. Geological Survey Geologic Investigations Series I-2766, scale 1:100,000.
- Billingsley, G.H., Beus, S.S., and Grover, P., 1999, Stratigraphy of the Surprise Canyon Formation, in Billingsley, G.H., and Beus, S.S., eds., *Geology of the Surprise Canyon Formation of the Grand Canyon, Arizona*: Northern Arizona Bulletin, v. 61, p. 9–16.
- Billingsley, G.H., Block, D.L., and Dyer, H.C., 2006a, Geological map of the Peach Springs 30' × 60' quadrangle, Coconino County, northwestern Arizona: U.S. Geological Survey Geologic Investigations Series I-2895, scale 1:100,000.
- Billingsley, G.H., Felger, T.J., and Priest, S.S., 2006b, Geological map of the Valle 30' × 60' quadrangle, Coconino County, northern Arizona: U.S. Geological Survey Geologic Investigations Series I-2895, scale 1:100,000.
- Billingsley, G.H., Priest, S.S., and Felger, T.J., 2007, Geological map of the Cameron 30' × 60' quadrangle, Coconino County, northern Arizona: U.S. Geological Survey Geologic Investigations Series I-2977, scale 1:100,000.
- Billingsley, T.J., Stoffer, P.W., and Priest, S.S., 2012, Geological map of the Tuba City 30' × 60' quadrangle, Coconino County, northern Arizona: U.S. Geological Survey Scientific Investigations Map 3227, scale 1:50,000, 3 sheets, 12 p. text, <https://doi.org/10.3133/sim3227>.
- Bird, P., 1979, Continental delamination and the Colorado Plateau: *Journal of Geophysical Research: Solid Earth*, v. 84, no. B13, p. 7561–7571, <https://doi.org/10.1029/JB084iB13p07561>.
- Bishop, J.W., Montañez, I.P., Gulbranson, E.L., and Brenckle, P.L., 2009, The onset of mid-Carboniferous glacio-eustasy: Sedimentologic and diagenetic constraints, Arrow Canyon, Nevada: *Palaeogeography, Palaeoclimatology, Palaeoecology*, v. 276, p. 217–243, <https://doi.org/10.1016/j.palaeo.2009.02.019>.
- Bishop, J.W., Montañez, I.P., and Osleger, D.A., 2010, Dynamic Carboniferous climate change, Arrow Canyon, Nevada: *Geosphere*, v. 6, no. 1, p. 1–34, <https://doi.org/10.1130/GES00192.1>.
- Blake, B.M.Jr., and Beuthin, J.D., 2008, Deciphering the mid-Carboniferous eustatic event in the central Appalachian foreland basin, southern West Virginia, USA, in Fielding, C.R., Frank, T.D., and Isbell, J.L., *Resolving the Late Paleozoic Ice Age in Space and Time: Geological Society of America Special Paper 441*, p. 249–260, [https://doi.org/10.1130/2008.2441\(17\)](https://doi.org/10.1130/2008.2441(17)).
- Blakey, R.C., 2003, Supai Group and Hermit Formation, in Beus, S.S., and Morales, M., eds., *Grand Canyon Geology* (2nd edition): New York, USA, Oxford University Press, p. 136–162.
- Blakey, R.C., and Knepp, R., 1989, Pennsylvanian and Permian geology of Arizona, in Jenney, J.P., and Reynolds, S.J., eds., *Geologic Evolution of Arizona: Arizona Geological Society Digest*, v. 17, p. 313–347.
- Bond, G.C., Kominz, M.A., and Devlin, W.J., 1983, Thermal subsidence and eustasy in the Lower Palaeozoic miogeocline of western North America: *Nature*, v. 306, p. 775–779, <https://doi.org/10.1038/306775a0>.
- Bond, G.C., Christie-Blick, N., Kominz, M.A., and Devlin, W.J., 1985, An early Cambrian rift to post-rift transition in the Cordillera of western North America: *Nature*, v. 315, p. 742–746, <https://doi.org/10.1038/315742a0>.
- Brezinski, D.K., 2017, Trilobites from the Redwall Limestone (Mississippian) of Arizona: *Annals of the Carnegie Museum*, v. 84, p. 165–171, <https://doi.org/10.2992/007.084.0202>.
- Bristol, H.M., and Howard, R.H., 1971, Paleogeographic map of the sub-Pennsylvanian Chesterian (upper Mississippian) surface in the Illinois Basin: *Illinois State Geological Survey Circular 458*, 16 p.
- Bunge, H.P., Hagelberg, C.R., and Travis, B.J., 2003, Mantle circulation models with variational data assimilation: Inferring mantle flow and structure from plate motion histories and seismic tomography: *Geophysical Journal International*, v. 152, p. 280–301, <https://doi.org/10.1046/j.1365-246X.2003.01823.x>.
- Burke, K., 1996, The African plate: *South African Journal of Geology*, v. 99, no. 4, p. 341–409.
- Carslaw, H.S., and Jaeger, J.C., 1959, *Conduction of Heat in Solids* (2nd edition): Oxford, UK, Oxford University Press, 510 p.
- Cazenave, A., Dominik, K., Allegre, C.J., and Marsh, J.G., 1986, Global relationship between oceanic geoid and topography: *Journal of Geophysical Research: Solid Earth*, v. 91, no. B11, p. 11,439–11,450, <https://doi.org/10.1029/JB091iB11p11439>.
- Cazenave, A., Dominik, K., Rabinowicz, M., and Ceuleneer, G., 1988, Geoid and depth anomalies over ocean swells and troughs: Evidence of an increasing trend of the geoid to depth ratio with age of plate: *Journal of Geophysical Research: Solid Earth*, v. 93, no. B7, p. 8064–8077, <https://doi.org/10.1029/JB093iB07p08064>.
- Cochran, J.R., and Talwani, M., 1977, Free-air gravity anomalies in the world's oceans and their relationship to residual elevation: *Geophysical Journal International*, v. 50, no. 3, p. 495–552, <https://doi.org/10.1111/j.1365-246X.1977.tb01334.x>.
- Colli, L., Ghelichkhan, S., and Bunge, H.-P., 2016, On the ratio of dynamic topography and gravity anomalies in a dynamic Earth: *Geophysical Research Letters*, v. 43, no. 6, p. 2510–2516, <https://doi.org/10.1002/2016GL067929>.
- Colpron, M., and Nelson, J.L., 2009, A Paleozoic northwest passage: Incursion of Caledonian, Baltic and Siberian terranes into eastern Panthalassa, and the early evolution of the North American Cordilleran, in Cawood, P.A., and Kröner, A., eds., *Earth Accretionary Systems in Space and Time: Geological Society, London, Special Publication 318*, p. 273–307, <https://doi.org/10.1144/SP318.10>.
- Conrad, C.P., and Gurnis, M., 2003, Seismic tomography, surface uplift, and the breakup of Gondwanaland: Integrating mantle convection backwards in time: *Geodynamics, Geophysics, Geosystems*, v. 4, no. 3, <https://doi.org/10.1029/2001GC000299>.
- Czarnota, K., Hoggard, M.J., White, N.J., and Winterbourne, J., 2013, Spatial and temporal patterns of Cenozoic

- dynamic topography around Australia: Geochemistry, Geophysics, Geosystems, v. 14, no. 3, p. 634–658, <https://doi.org/10.1029/2012GC004392>.
- Dam, G., 2002, Sedimentology of magmatically and structurally controlled outburst valleys along rifted volcanic margins: Examples from the Nuussuaq Basin, West Greenland: *Sedimentology*, v. 49, p. 505–532, <https://doi.org/10.1046/j.1365-3091.2002.00457.x>.
- Davies, D.R., Valentine, A.P., Kramer, S.C., Rawlinson, N., Hoggard, M.J., Eakin, C.M., and Wilson, C.R., 2019, Earth's multi-scale topographic response to global mantle flow: *Nature Geoscience*, v. 12, p. 845–850, <https://doi.org/10.1038/s41561-019-0441-4>.
- Davies, G.F., 1994, Thermomechanical erosion of the lithosphere by mantle plumes: *Journal of Geophysical Research: Solid Earth*, v. 99, no. B8, p. 15,709–15,722, <https://doi.org/10.1029/94JB00119>.
- Davydov, V.I., Korn, D., and Schmitz, M.D., 2012, The Carboniferous Period, in *Gradstein, F.M., Ogg, J.G., Schmitz, M.D. and Ogg, G.*, eds., *The Geologic Time Scale*: Amsterdam, Elsevier, p. 603–651, <https://doi.org/10.1016/B978-0-444-59425-9.00023-8>.
- De Voto, R.H., 1988, Late Mississippian paleokarst and related mineral deposits, Leadville Formation, Central Colorado, in *James, N.P., and Choquette, P.W.*, *Paleokarst*: New York, Springer-Verlag, p. 278–305, https://doi.org/10.1007/978-1-4612-3748-8_14.
- Dehler, C., Gehrels, G., Porter, S., Heizler, M., Karlstrom, K., Cox, G., Crossey, L., and Timmons, M., 2017, Synthesis of the 780–740 Ma Chuar, Uinta Mountain and Pahrum (ChUMP) groups, western USA: Implications for Laurentia-wide cratonic marine basins: *Geological Society of America Bulletin*, v. 129, no. 5/6, p. 607–624, <https://doi.org/10.1130/B31532.1>.
- Dickinson, W.R., 2004, Evolution of the North American Cordillera: Annual Review of Earth and Planetary Sciences, v. 32, p. 13–45, <https://doi.org/10.1146/annurev.earth.32.101802.120257>.
- Dickinson, W.R., and Lawton, T.F., 2003, Sequential intercontinental suturing as the ultimate control for Pennsylvanian Ancestral Rocky Mountains deformation: *Geology*, v. 31, no. 7, p. 609–612, [https://doi.org/10.1130/0091-7613\(2003\)031<0609:SISATU>2.0.CO;2](https://doi.org/10.1130/0091-7613(2003)031<0609:SISATU>2.0.CO;2).
- Droste, J.B., and Keller, S.J., 1989, Development of the Mississippian-Pennsylvanian unconformity in Indiana: *Indiana Geological Survey Occasional Paper* 55, 11 p.
- Dumitru, T.A., Duddy, I.R., and Green, P.F., 1994, Mesozoic-Cenozoic burial, uplift, and erosion history of the west-central Colorado Plateau: *Geology*, v. 22, p. 499–502, [https://doi.org/10.1130/0091-7613\(1994\)022<0499:MCBUA>2.3.CO;2](https://doi.org/10.1130/0091-7613(1994)022<0499:MCBUA>2.3.CO;2).
- Dyer, B., Maloof, A.C., and Higgins, J.A., 2015, Glacioeustasy, meteoric diagenesis, and the carbon cycle during the Middle Carboniferous: *Geochemistry, Geophysics, Geosystems*, v. 16, p. 3383–3399, <https://doi.org/10.1002/2015GC006002>.
- Ettensohn, F.R., 1994, Tectonic control on formation and cyclicity of major Appalachian unconformities and associated stratigraphic sequences, in *Dennison, J.M., and Ettensohn, F.R.*, eds., *Tectonic and Eustatic Controls of Sedimentary Cycles*: Tulsa, Oklahoma, USA, SEPM (Society for Sedimentary Geology), p. 217–241, <https://doi.org/10.2110/csp.94.04.0207>.
- Fielding, C.R., Frank, T.D., and Isbell, J.L., 2008, The late Paleozoic ice age—A review of current understanding and synthesis of global climate patterns, in *Fielding, C.R., Frank, T.D., and Isbell, J.L.*, Resolving the Late Paleozoic Ice Age in Space and Time: *Geological Society of America Special Paper* 441, p. 343–354, [https://doi.org/10.1130/2008.2441\(24\)](https://doi.org/10.1130/2008.2441(24)).
- Fittion, J.G., James, D., and Leeman, W.P., 1991, Basic magmatism associated with Late Cenozoic extension in the Western United States: Compositional variations in space and time: *Journal of Geophysical Research: Solid Earth*, v. 96, no. B8, p. 13,693–13,711, <https://doi.org/10.1029/91JB00372>.
- Flament, N., Gurnis, M., and Müller, R.D., 2013, A review of observations and models of dynamic topography: *Lithosphere*, v. 5, no. 2, p. 189–210, <https://doi.org/10.1130/L245.1>.
- Ford, T.D., and Dehler, C.M., 2003, Grand Canyon Supergroup: Nankoweap Formation, Chuar Group, in *Beus, S.S., and Morales, M.*, eds., *Grand Canyon Geology* (2nd edition): New York, USA, Oxford University Press, p. 53–75.
- Gehrels, G.E., Blakey, R., Karlstrom, K.E., Timmons, J.M., Dickinson, B., and Pecha, M., 2011, Detrital zircon U-Pb geochronology of paleozoic strata in the Grand Canyon, Arizona: *Lithosphere*, v. 3, no. 3, p. 183–200, <https://doi.org/10.1130/L121.1>.
- Giles, K.A., and Dickinson, W.R., 1995, The interplay of eustasy and lithospheric flexure in forming the stratigraphic sequences in foreland settings: An example from the Antler Foreland, Nevada and Utah: *Society of Economic Paleontologists and Mineralogists Special Publication* 52, p. 187–211, <https://doi.org/10.2110/pec.95.52.0187>.
- Grossman, E.L., Yancey, T.E., Bruckschen, P., Chuvashov, B., Mazzullo, S.J., and Mii, H.-S., 2008, Glaciation, aridification, and carbon sequestration in the Permo-Carboniferous: The isotopic record from low latitudes: *Palaeogeography, Palaeoclimatology, Palaeoecology*, v. 268, no. 3–4, p. 222–233, <https://doi.org/10.1016/j.palaeo.2008.03.053>.
- Grover, P.W., 1989, Stratigraphy and depositional environment of the Surprise Canyon Formation, and upper Mississippian carbonate-clastic estuarine deposit, Grand Canyon, Arizona [M.S. dissertation]: Flagstaff, Arizona, USA, Northern Arizona University, 303 p.
- Gunn, R., 1943, A quantitative evaluation of the influence of the lithosphere on the anomalies of gravity: *Journal of the Franklin Institute*, v. 236, p. 47–65, [https://doi.org/10.1016/S0016-0032\(43\)91198-6](https://doi.org/10.1016/S0016-0032(43)91198-6).
- Gutschick, R.C., and Sandberg, C.A., 1983, Mississippian continental margins of the conterminous United States: *Society of Economic Paleontologists and Mineralogists Special Publication* 33, p. 79–96, <https://doi.org/10.2110/pec.83.06.0079>.
- Hager, B.H., and Richards, M.A., 1989, Long-wavelength variations in Earth's geoid: Physical models and dynamical implications: *Philosophical Transactions of the Royal Society of London. Series A, Mathematical and Physical Sciences*, v. 328, no. 1599, p. 309–327, <https://doi.org/10.1098/rsta.1989.0038>.
- Hartley, R.A., Roberts, G.G., White, N., and Richardson, C., 2011, Transient convective uplift of an ancient buried landscape: *Nature Geoscience*, v. 4, no. 8, p. 562–565, <https://doi.org/10.1038/ngeo1191>.
- Hartley, R.W., and Allen, P.A., 1994, Interior cratonic basins of Africa: Relation to continental break-up and role of mantle convection: *Basin Research*, v. 6, no. 2–3, p. 95–113, <https://doi.org/10.1111/j.1365-2117.1994.tb0078.x>.
- Hautmann, M., Smith, A.B., McGowan, A.J., and Bucher, H., 2013, Bivalves from the Olenekian (Early Triassic) of south-western Utah: Systematics and evolutionary significance: *Journal of Systematic Palaeontology*, v. 11, no. 3, p. 263–293, <https://doi.org/10.1080/14772019.2011.637516>.
- Hendricks, J.D., and Stevenson, G.M., 2003, Grand Canyon Supergroup: Unkar Group, in *Beus, S.S., and Morales, M.*, eds., *Grand Canyon Geology* (2nd edition): New York, USA, Oxford University Press, p. 39–52.
- Hintze, L.F., 1988, *Geologic History of Utah*: Provo, Utah, USA, Department of Geology, Brigham Young University, 181 p.
- Hoggard, M.J., White, N., and Al-Attar, D., 2016, Global dynamic topography observations reveal limited influence of large-scale mantle flow: *Nature Geoscience*, v. 9, p. 456–463, <https://doi.org/10.1038/ngeo2709>.
- Hoggard, M.J., Winterbourne, J., Czarnota, K., and White, N., 2017, Oceanic residual depth measurements, the plate cooling model and global dynamic topography: *Journal of Geophysical Research: Solid Earth*, v. 122, no. 3, p. 2328–2372, <https://doi.org/10.1002/2016JB013457>.
- Hopkins, R.L., and Thompson, K.L., 2003, Kaibab Formation, in *Beus, S.S., and Morales, M.*, eds., *Grand Canyon Geology* (2nd edition): New York, USA, Oxford University Press, p. 196–212.
- Horton, D.E., Poulsen, C.J., and Pollard, D., 2010, Influence of high-latitude vegetation feedbacks on late Paleozoic glacial cycles: *Nature Geoscience*, v. 3, p. 572–577, <https://doi.org/10.1038/ngeo2709>.
- Horton, D.E., Poulsen, C.J., Montañez, I., and DiMichele, W.A., 2012, Eccentricity-paced late Paleozoic climate change: *Palaeogeography, Palaeoclimatology, Palaeoecology*, v. 331–332, p. 150–161, <https://doi.org/10.1016/j.palaeo.2012.03.014>.
- Howard, R.H., and Whitaker, S.T., 1988, Hydrocarbon accumulation in a paleovalley at Mississippian-Pennsylvanian unconformity near Hardinville, Crawford County, Illinois: A model paleogeomorphic trap: Department of Energy and Natural Resources, Illinois State Geological Survey, Illinois Petroleum 129, 34 p.
- Jones, S.M., White, N., and Lovell, B., 2001, Cenozoic and Cretaceous transient uplift in the Porcupine Basin and its relationship to a mantle plume, in *Shannon, P.M., Haughton, P.D.W., and Corcoran, D.V.*, eds., *The Petroleum Exploration of Ireland's Offshore Basins*: Geological Society, London, Special Publication 188, p. 345–360, <https://doi.org/10.1144/GSL.SP.2001.188.01.20>.
- Karlstrom, K.E., and Bowring, S.A., 1993, Proterozoic orogenic history of Arizona, in *Van Schmus, W.R., and Bickford, M.E.*, eds., *Transcontinental Proterozoic Provinces, Precambrian: Conterminous U.S.*: Boulder, Colorado, USA, Geological Society of America, *Geology of North America*, v. C-2, p. 188–211, <https://doi.org/10.1130/DNAG-GNA-C2.171>.
- Karlstrom, K.E., Bowring, S.A., Dehler, C.M., Knoll, A.H., Porter, S.M., Des Marais, D.J., Weil, A.B., Sharp, Z.D., Geissman, J.W., Elrick, M.B., Timmons, J.M., Crossey, L.J., and Davidek, K.L., 2000, Chuar Group of the Grand Canyon: Record of breakup of Rodinia, associated change in the global carbon cycle, and ecosystem expansion by 740 Ma: *Geology*, v. 28, no. 7, p. 619–622, [https://doi.org/10.1130/0091-7613\(2000\)28<619:CGO>2.0.CO;2](https://doi.org/10.1130/0091-7613(2000)28<619:CGO>2.0.CO;2).
- Karlstrom, K.E., Coblenz, D., Dueker, K., Ouimet, W., Kirby, E., van Wijk, J., Schmandt, B., Kelley, S., Lazear, G., Crossey, L.J., Crow, R., Aslan, A., Darling, A., Aster, R., MacCarthy, J., Hansen, S.M., Stachnik, J., Stockli, D.F., Garcia, R.V., Hoffman, M., McKeon, R., Feldman, J., Heizler, M., and Donahue, M.S., and the CREST Working Group, 2012, Mantle-driven dynamic uplift of the Rocky Mountains and Colorado Plateau and its surface response: Toward a unified hypothesis: *Lithosphere*, v. 4, no. 1, p. 3–22, <https://doi.org/10.1130/L150.1>.
- Karlstrom, K.E., Hagadorn, J., Gehrels, G., Matthews, W., Schmitz, M., Madronich, L., Mulder, J., Pecha, M., Giesler, D., and Crossey, L., 2018, Cambrian Sauk transgression in the Grand Canyon region redefined by detrital zircons: *Nature Geoscience*, v. 11, p. 438–443, <https://doi.org/10.1038/s41561-018-0131-7>.
- Kent, W.N., and Rawson, R.R., 1980, Depositional environments of the Mississippian Redwall Limestone in north-eastern Arizona, in *Fouch, T.D., and Magathan, E.R.*, *Paleozoic Paleogeography of the West-Central United States: Proceedings of the Rocky Mountain Symposium 1*, Society of Economic Paleontologists and Mineralogists, p. 101–109.
- Klöcking, M., White, N.J., MacLennan, J., McKenzie, D., and Fitton, J.G., 2018, Quantitative relationships between basalt geochemistry, shear wave velocity, and asthenospheric temperature beneath western North America: *Geochemistry, Geophysics, Geosystems*, v. 19, no. 9, p. 3376–3404, <https://doi.org/10.1029/2018GC007559>.
- Kluth, C.F., and Coney, P.J., 1981, Plate tectonics of the Ancestral Rocky Mountains: *Geology*, v. 9, p. 10–15, [https://doi.org/10.1130/0091-7613\(1981\)9<10:PTOTA>2.0.CO;2](https://doi.org/10.1130/0091-7613(1981)9<10:PTOTA>2.0.CO;2).
- Korn, D., 2006, Ammonoïdei, in *Deutsche Stratigraphie Kommission*, eds., *Stratigraphie von Deutschland VI. Unterkarbon (Mississippium)*. Schriftenreihe der Deutschen Gesellschaft für Geowissenschaften 41: Hannover, Germany, Deutsche Gesellschaft für Geowissenschaften, p. 147–170.
- Lane, H.R., and Brenckle, P.L., 2005, Type Mississippian subdivisions and biostratigraphic succession, in *Heckel, P.H.*, ed., *Stratigraphy and Biostratigraphy of the Mississippian Subsystem (Carboniferous System) in Its Type Region, the Mississippi River Valley of Illinois, Missouri and Iowa*: Champaign, Illinois, USA, Illinois State Geological Survey, p. 76–105.
- Lane, H.R., and Brenckle, P.L., 2005, Type Mississippian subdivisions and biostratigraphic succession, in *Heckel, P.H.*, ed., *Stratigraphy and Biostratigraphy of the Mississippian Subsystem (Carboniferous System) in Its Type Region, the Mississippi River Valley of Illinois, Missouri and Iowa*: Champaign, Illinois, USA, Illinois State Geological Survey, p. 76–105.
- Lane, H.R., and Brenckle, P.L., 2005, Type Mississippian subdivisions and biostratigraphic succession, in *Heckel, P.H.*, ed., *Stratigraphy and Biostratigraphy of the Mississippian Subsystem (Carboniferous System) in Its Type Region, the Mississippi River Valley of Illinois, Missouri and Iowa*: Champaign, Illinois, USA, Illinois State Geological Survey, p. 76–105.
- Lane, H.R., and Brenckle, P.L., 2005, Type Mississippian subdivisions and biostratigraphic succession, in *Heckel, P.H.*, ed., *Stratigraphy and Biostratigraphy of the Mississippian Subsystem (Carboniferous System) in Its Type Region, the Mississippi River Valley of Illinois, Missouri and Iowa*: Champaign, Illinois, USA, Illinois State Geological Survey, p. 76–105.
- Lane, H.R., and Brenckle, P.L., 2005, Type Mississippian subdivisions and biostratigraphic succession, in *Heckel, P.H.*, ed., *Stratigraphy and Biostratigraphy of the Mississippian Subsystem (Carboniferous System) in Its Type Region, the Mississippi River Valley of Illinois, Missouri and Iowa*: Champaign, Illinois, USA, Illinois State Geological Survey, p. 76–105.
- Lane, H.R., and Brenckle, P.L., 2005, Type Mississippian subdivisions and biostratigraphic succession, in *Heckel, P.H.*, ed., *Stratigraphy and Biostratigraphy of the Mississippian Subsystem (Carboniferous System) in Its Type Region, the Mississippi River Valley of Illinois, Missouri and Iowa*: Champaign, Illinois, USA, Illinois State Geological Survey, p. 76–105.
- Lane, H.R., and Brenckle, P.L., 2005, Type Mississippian subdivisions and biostratigraphic succession, in *Heckel, P.H.*, ed., *Stratigraphy and Biostratigraphy of the Mississippian Subsystem (Carboniferous System) in Its Type Region, the Mississippi River Valley of Illinois, Missouri and Iowa*: Champaign, Illinois, USA, Illinois State Geological Survey, p. 76–105.
- Lane, H.R., and Brenckle, P.L., 2005, Type Mississippian subdivisions and biostratigraphic succession, in *Heckel, P.H.*, ed., *Stratigraphy and Biostratigraphy of the Mississippian Subsystem (Carboniferous System) in Its Type Region, the Mississippi River Valley of Illinois, Missouri and Iowa*: Champaign, Illinois, USA, Illinois State Geological Survey, p. 76–105.
- Lane, H.R., and Brenckle, P.L., 2005, Type Mississippian subdivisions and biostratigraphic succession, in *Heckel, P.H.*, ed., *Stratigraphy and Biostratigraphy of the Mississippian Subsystem (Carboniferous System) in Its Type Region, the Mississippi River Valley of Illinois, Missouri and Iowa*: Champaign, Illinois, USA, Illinois State Geological Survey, p. 76–105.
- Lane, H.R., and Brenckle, P.L., 2005, Type Mississippian subdivisions and biostratigraphic succession, in *Heckel, P.H.*, ed., *Stratigraphy and Biostratigraphy of the Mississippian Subsystem (Carboniferous System) in Its Type Region, the Mississippi River Valley of Illinois, Missouri and Iowa*: Champaign, Illinois, USA, Illinois State Geological Survey, p. 76–105.
- Lane, H.R., and Brenckle, P.L., 2005, Type Mississippian subdivisions and biostratigraphic succession, in *Heckel, P.H.*, ed., *Stratigraphy and Biostratigraphy of the Mississippian Subsystem (Carboniferous System) in Its Type Region, the Mississippi River Valley of Illinois, Missouri and Iowa*: Champaign, Illinois, USA, Illinois State Geological Survey, p. 76–105.
- Lane, H.R., and Brenckle, P.L., 2005, Type Mississippian subdivisions and biostratigraphic succession, in *Heckel, P.H.*, ed., *Stratigraphy and Biostratigraphy of the Mississippian Subsystem (Carboniferous System) in Its Type Region, the Mississippi River Valley of Illinois, Missouri and Iowa*: Champaign, Illinois, USA, Illinois State Geological Survey, p. 76–105.
- Lane, H.R., and Brenckle, P.L., 2005, Type Mississippian subdivisions and biostratigraphic succession, in *Heckel, P.H.*, ed., *Stratigraphy and Biostratigraphy of the Mississippian Subsystem (Carboniferous System) in Its Type Region, the Mississippi River Valley of Illinois, Missouri and Iowa*: Champaign, Illinois, USA, Illinois State Geological Survey, p. 76–105.
- Lane, H.R., and Brenckle, P.L., 2005, Type Mississippian subdivisions and biostratigraphic succession, in *Heckel, P.H.*, ed., *Stratigraphy and Biostratigraphy of the Mississippian Subsystem (Carboniferous System) in Its Type Region, the Mississippi River Valley of Illinois, Missouri and Iowa*: Champaign, Illinois, USA, Illinois State Geological Survey, p. 76–105.
- Lane, H.R., and Brenckle, P.L., 2005, Type Mississippian subdivisions and biostratigraphic succession, in *Heckel, P.H.*, ed., *Stratigraphy and Biostratigraphy of the Mississippian Subsystem (Carboniferous System) in Its Type Region, the Mississippi River Valley of Illinois, Missouri and Iowa*: Champaign, Illinois, USA, Illinois State Geological Survey, p. 76–105.
- Lane, H.R., and Brenckle, P.L., 2005, Type Mississippian subdivisions and biostratigraphic succession, in *Heckel, P.H.*, ed., *Stratigraphy and Biostratigraphy of the Mississippian Subsystem (Carboniferous System) in Its Type Region, the Mississippi River Valley of Illinois, Missouri and Iowa*: Champaign, Illinois, USA, Illinois State Geological Survey, p. 76–105.
- Lane, H.R., and Brenckle, P.L., 2005, Type Mississippian subdivisions and biostratigraphic succession, in *Heckel, P.H.*, ed., *Stratigraphy and Biostratigraphy of the Mississippian Subsystem (Carboniferous System) in Its Type Region, the Mississippi River Valley of Illinois, Missouri and Iowa*: Champaign, Illinois, USA, Illinois State Geological Survey, p. 76–105.
- Lane, H.R., and Brenckle, P.L., 2005, Type Mississippian subdivisions and biostratigraphic succession, in *Heckel, P.H.*, ed., *Stratigraphy and Biostratigraphy of the Mississippian Subsystem (Carboniferous System) in Its Type Region, the Mississippi River Valley of Illinois, Missouri and Iowa*: Champaign, Illinois, USA, Illinois State Geological Survey, p. 76–105.
- Lane, H.R., and Brenckle, P.L., 2005, Type Mississippian subdivisions and biostratigraphic succession, in *Heckel, P.H.*, ed., *Stratigraphy and Biostratigraphy of the Mississippian Subsystem (Carboniferous System) in Its Type Region, the Mississippi River Valley of Illinois, Missouri and Iowa*: Champaign, Illinois, USA, Illinois State Geological Survey, p. 76–105.
- Lane, H.R., and Brenckle, P.L., 2005, Type Mississippian subdivisions and biostratigraphic succession, in *Heckel, P.H.*, ed., *Stratigraphy and Biostratigraphy of the Mississippian Subsystem (Carboniferous System) in Its Type Region, the Mississippi River Valley of Illinois, Missouri and Iowa*: Champaign, Illinois, USA, Illinois State Geological Survey, p. 76–105.
- Lane, H.R., and Brenckle, P.L., 2005, Type Mississippian subdivisions and biostratigraphic succession, in *Heckel, P.H.*, ed., *Stratigraphy and Biostratigraphy of the Mississippian Subsystem (Carboniferous System) in Its Type Region, the Mississippi River Valley of Illinois, Missouri and Iowa*: Champaign, Illinois, USA, Illinois State Geological Survey, p. 76–105.
- Lane, H.R., and Brenckle, P.L., 2005, Type Mississippian subdivisions and biostratigraphic succession, in *Heckel, P.H.*, ed., *Stratigraphy and Biostratigraphy of the Mississippian Subsystem (Carboniferous System) in Its Type Region, the Mississippi River Valley of Illinois, Missouri and Iowa*: Champaign, Illinois, USA, Illinois State Geological Survey, p. 76–105.
- Lane, H.R., and Brenckle, P.L., 2005, Type Mississippian subdivisions and biostratigraphic succession, in *Heckel, P.H.*, ed., *Stratigraphy and Biostratigraphy of the Mississippian Subsystem (Carboniferous System) in Its Type Region, the Mississippi River Valley of Illinois, Missouri and Iowa*: Champaign, Illinois, USA, Illinois State Geological Survey, p. 76–105.
- Lane, H.R., and Brenckle, P.L., 2005, Type Mississippian subdivisions and biostratigraphic succession, in *Heckel, P.H.*, ed., *Stratigraphy and Biostratigraphy of the Mississippian Subsystem (Carboniferous System) in Its Type Region, the Mississippi River Valley of Illinois, Missouri and Iowa*: Champaign, Illinois, USA, Illinois State Geological Survey, p. 76–105.
- Lane, H.R., and Brenckle, P.L., 2005, Type Mississippian subdivisions and biostratigraphic succession, in *Heckel, P.H.*, ed., *Stratigraphy and Biostratigraphy of the Mississippian Subsystem (Carboniferous System) in Its Type Region, the Mississippi River Valley of Illinois, Missouri and Iowa*: Champaign, Illinois, USA, Illinois State Geological Survey, p. 76–105.
- Lane, H.R., and Brenckle, P.L., 2005, Type Mississippian subdivisions and biostratigraphic succession, in *Heckel, P.H.*, ed., *Stratigraphy and Biostratigraphy of the Mississippian Subsystem (Carboniferous System) in Its Type Region, the Mississippi River Valley of Illinois, Missouri and Iowa*: Champaign, Illinois, USA, Illinois State Geological Survey, p. 76–105.
- Lane, H.R., and Brenckle, P.L., 2005, Type Mississippian subdivisions and biostratigraphic succession, in *Heckel, P.H.*, ed., *Stratigraphy and Biostratigraphy of the Mississippian Subsystem (Carboniferous System) in Its Type Region, the Mississippi River Valley of Illinois, Missouri and Iowa*: Champaign, Illinois, USA, Illinois State Geological Survey, p. 76–105.
- Lane, H.R., and Brenckle, P.L., 2005, Type Mississippian subdivisions and biostratigraphic succession, in *Heckel, P.H.*, ed., *Stratigraphy and Biostratigraphy of the Mississippian Subsystem (Carboniferous System) in Its Type Region, the Mississippi River Valley of Illinois, Missouri and Iowa*: Champaign, Illinois, USA, Illinois State Geological Survey, p. 76–105.
- Lane, H.R., and Brenckle, P.L., 2005, Type Mississippian subdivisions and biostratigraphic succession, in *Heckel, P.H.*, ed., *Stratigraphy and Biostratigraphy of the Mississippian Subsystem (Carboniferous System) in Its Type Region, the Mississippi River Valley of Illinois, Missouri and Iowa*: Champaign, Illinois, USA, Illinois State Geological Survey, p. 76–105.
- Lane, H.R., and Brenckle, P.L., 2005, Type Mississippian subdivisions and biostratigraphic succession, in *Heckel, P.H.*, ed., *Stratigraphy and Biostratigraphy of the Mississippian Subsystem (Carboniferous System) in Its Type Region, the Mississippi River Valley of Illinois, Missouri and Iowa*: Champaign, Illinois, USA, Illinois State Geological Survey, p. 76–105.
- Lane, H.R., and Brenckle, P.L., 2005, Type Mississippian subdivisions and biostratigraphic succession, in *Heckel, P.H.*, ed., *Stratigraphy and Biostratigraphy of the Mississippian Subsystem (Carboniferous System) in Its Type Region, the Mississippi River Valley of Illinois, Missouri and Iowa*: Champaign, Illinois, USA, Illinois State Geological Survey, p. 76–105.
- Lane, H.R., and Brenckle, P.L., 2005, Type Mississippian subdivisions and biostratigraphic succession, in *Heckel, P.H.*, ed., *Stratigraphy and Biostratigraphy of the Mississippian Subsystem (Carboniferous System) in Its Type Region, the Mississippi River Valley of Illinois, Missouri and Iowa*: Champaign, Illinois, USA, Illinois State Geological Survey, p. 76–105.
- Lane, H.R., and Brenckle, P.L., 2005, Type Mississippian subdivisions and biostratigraphic succession, in *Heckel, P.H.*, ed., *Stratigraphy and Biostratigraphy of the Mississippian Subsystem (Carboniferous System) in Its Type Region, the Mississippi River Valley of Illinois, Missouri and Iowa*: Champaign, Illinois, USA, Illinois State Geological Survey, p. 76–105.
- Lane, H.R., and Brenckle, P.L., 2005, Type Mississippian subdivisions and biostratigraphic succession, in *Heckel, P.H.*, ed., *Stratigraphy and Biostratigraphy of the Mississippian Subsystem (Carboniferous System) in Its Type Region, the Mississippi River Valley of Illinois, Missouri and Iowa*: Champaign, Illinois, USA, Illinois State Geological Survey, p. 76–105.
- Lane, H.R., and Brenckle, P.L., 2005, Type Mississippian subdivisions and biostratigraphic succession, in *Heckel, P.H.*, ed., *Stratigraphy and Biostratigraphy of the Mississippian Subsystem (Carboniferous System) in Its Type Region, the Mississippi River Valley of Illinois, Missouri and Iowa*: Champaign, Illinois, USA, Illinois State Geological Survey, p. 76–105.
- Lane, H.R., and Brenckle, P.L., 2005, Type Mississippian subdivisions and biostratigraphic succession, in *Heckel, P.H.*, ed., *Stratigraphy and Biostratigraphy of the Mississippian Subsystem (Carboniferous System) in Its Type Region, the Mississippi River Valley of Illinois, Missouri and Iowa*: Champaign, Illinois, USA, Illinois State Geological Survey, p. 76–105.
- Lane, H.R., and Brenckle, P.L., 2005, Type Mississippian subdivisions and biostratigraphic succession, in *Heckel, P.H.*, ed., *Stratigraphy and Biostratigraphy of the Mississippian Subsystem (Carboniferous System) in Its Type Region, the Mississippi River Valley of Illinois, Missouri and Iowa*: Champaign, Illinois, USA, Illinois State Geological Survey, p. 76–105.
- Lane, H.R., and Brenckle, P.L., 2005, Type Mississippian subdivisions and biostratigraphic succession, in *Heckel, P.H.*, ed., *Stratigraphy and Biostratigraphy of the Mississippian Subsystem (Carboniferous System) in Its Type Region, the Mississippi River Valley of Illinois, Missouri and Iowa*: Champaign, Illinois, USA, Illinois State Geological Survey, p. 76–105.
- Lane, H.R., and Brenckle, P.L., 2005, Type Mississippian subdivisions and biostratigraphic succession, in *Heckel, P.H.*, ed., *Stratigraphy and Biostratigraphy of the Mississippian Subsystem (Carboniferous System) in Its Type Region, the Mississippi River Valley of Illinois, Missouri and Iowa*: Champaign, Illinois, USA, Illinois State Geological Survey, p. 76–105.
- Lane, H.R., and Brenckle, P.L., 2005, Type Mississippian subdivisions and biostratigraphic succession, in *Heckel, P.H.*, ed., *Stratigraphy and Biostratigraphy of the Mississippian Subsystem (Carboniferous System) in Its Type Region, the Mississippi River Valley of Illinois, Missouri and Iowa*: Champaign, Illinois, USA, Illinois State Geological Survey, p. 76–105.
- Lane, H.R., and Brenckle, P.L., 2005, Type Mississippian subdivisions and biostratigraphic succession, in *Heckel, P.H.*, ed., *Stratigraphy and Biostratigraphy of the Mississippian Subsystem (Carboniferous System) in Its Type Region, the Mississippi River Valley of Illinois, Missouri and Iowa*: Champaign, Illinois, USA, Illinois State Geological Survey, p. 76–105.
- Lane, H.R., and Brenckle, P.L., 2005, Type Mississippian subdivisions and biostratigraphic succession, in *Heckel, P.H.*, ed., *Stratigraphy and Biostratigraphy of the Mississippian Subsystem (Carboniferous System) in Its Type Region, the Mississippi River Valley of Illinois, Missouri and Iowa*: Champaign, Illinois, USA, Illinois State Geological Survey, p. 76–105.
- Lane, H.R., and Brenckle, P.L., 2005, Type Mississippian subdivisions and biostratigraphic succession, in *Heckel, P.H.*, ed., *Stratigraphy and Biostratigraphy of the Mississippian Subsystem (Carboniferous System) in Its Type Region, the Mississippi River Valley of Illinois, Missouri and Iowa*: Champaign, Illinois, USA, Illinois State Geological Survey, p. 76–105.
- Lane, H.R., and Brenckle, P.L., 2005, Type Mississippian subdivisions and biostratigraphic succession, in *Heckel, P.H.*, ed., *Stratigraphy and Biostratigraphy of the Mississippian Subsystem (Carboniferous System) in Its Type Region, the Mississippi River Valley of Illinois, Missouri and Iowa*: Champaign, Illinois, USA, Illinois State Geological Survey, p. 76–105.
- Lane, H.R., and Brenckle, P.L., 2005, Type Mississippian subdivisions and biostratigraphic succession, in *Heckel, P.H.*, ed., *Stratigraphy and Biostratigraphy of the Miss*

- Lawton, T.F., Cashman, P.H., Trexler, J.H., Jr., and Taylor, W.J., 2017, The late Paleozoic Southwestern Laurentian Borderland: *Geology*, v. 45, no. 8, p. 675–678, <https://doi.org/10.1130/G39071.1>.
- Leary, R.J., Umhoefer, P., Smith, M.E., and Riggs, N., 2017, A three-sided orogen: A new tectonic model for Ancestral Rocky Mountain uplift and basin development: *Geology*, v. 45, no. 8, p. 735–738, <https://doi.org/10.1130/G39041.1>.
- Leary, R.J., Umhoefer, P., Smith, M.E., Smith, T.M., Saylor, J.E., Riggs, N., Burr, G., Lodes, E., Foley, D., Licht, A., Mueller, M.A., and Baird, C., 2020, Provenance of Pennsylvanian–Permian sedimentary rocks associated with the Ancestral Rocky Mountains orogeny in southwestern Laurentia: Implications for continental-scale Laurentian sediment transport systems: *Lithosphere*, v. 12, no. 1, p. 88–121, <https://doi.org/10.1130/L1115.1>.
- Levy, M., and Christie-Blick, N., 1991, Tectonic subsidence of the early Paleozoic passive continental margin in eastern California and southern Nevada: *Geological Society of America Bulletin*, v. 103, p. 1590–1606, [https://doi.org/10.1130/0016-7606\(1991\)103<1590:TSOTEP>2.3.CO;2](https://doi.org/10.1130/0016-7606(1991)103<1590:TSOTEP>2.3.CO;2).
- Lin, P.-Y.P., Gaherty, J.B., Jin, G., Collins, J.A., Lizarralde, D., Evans, R.L., and Hirth, G., 2016, High-resolution seismic constraints on flow dynamics in the oceanic asthenosphere: *Nature*, v. 535, p. 538–542, <https://doi.org/10.1038/nature18012>.
- Lucazeau, F., 2019, Analysis and mapping of an updated terrestrial heat flow data set: *Geochemistry, Geophysics, Geosystems*, v. 20, p. 4001–4024, <https://doi.org/10.1029/2019GC008389>.
- Mamet, B., and Skipp, B., 1970, Lower Carboniferous calcareous foraminifera: Preliminary zonation and stratigraphic implications for the Mississippian of North America: *Proceedings, Compte Rendu, Sixième Congrès International de Stratigraphie et de Géologie du Carbonifère*, v. 3, p. 1129–1146.
- Martin, H., 1992, Conodont biostratigraphy and paleoenvironment of the Surprise Canyon Formation (late Mississippian), Grand Canyon, Arizona [M.S. dissertation]: Flagstaff, Arizona, USA, Northern Arizona University, 298 p.
- Martin, H., and Barrick, J.E., 1999, Conodont biostratigraphy, in Billingsley, G.H., and Beus, S.S., eds., *Geology of the Surprise Canyon Formation of the Grand Canyon, Arizona: Northern Arizona Bulletin*, v. 61, p. 97–116.
- Maslyn, R.M., 1977, Fossil tower karst near Molas Lake, Colorado: *The Mountain Geologist*, v. 14, no. 1, p. 17–25.
- Matthews, K.J., Maloney, K.T., Zahirovic, S., Williams, S.E., Seton, M., and Müller, R.D., 2016, Global plate boundary evolution and kinematics since the late Paleozoic: *Global and Planetary Change*, v. 146, p. 226–250, <https://doi.org/10.1016/j.gloplacha.2016.10.002>.
- Maughan, E.K., 1984, Paleogeographic setting of Pennsylvanian Tyler Formation and relation to underlying Mississippian rocks in Montana and North Dakota: *American Association of Petroleum Geologists Bulletin*, v. 68, no. 2, p. 178–195.
- Maughan, E.K., and Roberts, A.E., 1967, Big Snowy and Amsden Groups and the Mississippian–Pennsylvanian boundary in Montana: *U.S. Geological Survey Professional Paper 554-B*, p. B1–B27, <https://doi.org/10.3133/pp554B>.
- McColloch, M.E., Gilmour, E.H., and Snyder, E.M., 1994, The order Fenestrata (Bryozoa) of the Torowep Formation (Permian): Southern Nevada: *Journal of Paleontology*, v. 68, no. 4, p. 746–762, <https://doi.org/10.1017/S0022336000026196>.
- McKee, E.D., 1963, Nomenclature for lithologic subdivisions of the Mississippian Redwall Limestone, Arizona: *U.S. Geological Survey Professional Paper 475-C*, no. 65, p. C21–C22.
- McKee, E.D., 1975, The Supai Group—Subdivision and nomenclature: *U.S. Geological Survey Bulletin* 1935-J, p. J1–J11.
- McKee, E.D., 1982, Erosion surfaces, in *The Supai Group of the Grand Canyon: U.S. Geological Survey Professional Paper 1173*, p. 155–176.
- McKee, E.D., and Gutschick, R.C., 1969, History of the Redwall Limestone of Northern Arizona: *Geological Society of America Memoir* 114, 8 p.
- Menard, H.W., 1973, Depth anomalies and the bobbing motion of drifting islands: *Journal of Geophysical Research*, v. 78, no. 23, p. 5128–5137, <https://doi.org/10.1029/JB078i023p05128>.
- Meyers, W.J., 1988, Pelokarstic features in Mississippian limestones, Wyoming, in James, N.P., and Choquette, P.W., *Paleokarst*: New York, Springer-Verlag, p. 307–328, https://doi.org/10.1007/978-1-4612-3748-8_15.
- Middleton, L.T., and Elliot, D.K., 2003, Tonto Group, in Beus, S.S., and Morales, M., eds., *Grand Canyon Geology* (2nd edition): New York, USA, Oxford University Press, p. 90–107.
- Middleton, L.T., Elliot, D.K., and Morales, M., 2003, Coconino Sandstone, in Beus, S.S., and Morales, M., eds., *Grand Canyon Geology* (2nd edition): New York, USA, Oxford University Press, p. 163–179.
- Mii, H.-S., Grossman, E.L., and Yancey, T.E., 1999, Carboniferous isotope stratigraphies of North America: Implications for Carboniferous paleoceanography and Mississippian glaciation: *Geological Society of America Bulletin*, v. 111, no. 7, p. 960–973, [https://doi.org/10.1130/0016-7606\(1999\)111<0960:CISONA>2.3.CO;2](https://doi.org/10.1130/0016-7606(1999)111<0960:CISONA>2.3.CO;2).
- Mii, H.-S., Grossman, E.L., Yancey, T.E., Chuvashov, B., and Egorov, A., 2001, Isotopic records of brachiopod shells from the Russian Platform—evidence for the onset of mid-Carboniferous glaciation: *Chemical Geology*, v. 175, p. 133–147, [https://doi.org/10.1016/S0009-2541\(00\)00366-1](https://doi.org/10.1016/S0009-2541(00)00366-1).
- Miller, E.L., Miller, M.M., Stevens, C.H., Wright, J.E., and Madrid, R., 1992, Late Paleozoic paleogeographic and tectonic evolution of the western U.S. Cordillera, in Burchfield, B.C., and Lipman, P.W., *The Cordilleran Orogen: Conterminous U.S.*: Boulder, Colorado, USA, Geological Society of America, *Geology of North America*, v. G-3, p. 57–106, <https://doi.org/10.1130/DNAG-GNA-G3.57>.
- Montañez, I.P., and Poulsen, C.J., 2013, The Late Paleozoic Ice Age: An evolving paradigm: *Annual Review of Earth and Planetary Sciences*, v. 41, p. 629–656, <https://doi.org/10.1146/annurev.earth.031208.100118>.
- Morris, M., Fernandes, V.M., and Roberts, G.G., 2020, Extricating dynamic topography from subsidence patterns: Examples from eastern North America's passive margin: *Earth and Planetary Science Letters*, v. 530, no. e115840, <https://doi.org/10.1016/j.epsl.2019.115840>.
- McKenzie, D., 2020, The structure of the lithosphere and upper mantle beneath the Eastern Mediterranean and Middle East: *Mediterranean Geoscience Reviews*, v. 2, p. 311–326, <https://doi.org/10.1007/s42990-020-00038-1>.
- Moucha, R., Forte, A.M., Mitrovica, J.X., Rowley, D.B., Quéré, S., Simmons, N.A., and Grand, S.P., 2008, Dynamic topography and long-term sea-level variations: There is no such thing as a stable continental platform: *Earth and Planetary Science Letters*, v. 271, p. 101–108, <https://doi.org/10.1016/j.epsl.2008.03.056>.
- McNab, F., Ball, P.W., Hoggard, M.J., and White, N.J., 2018, Neogene uplift and magmatism of Anatolia: Insights from drainage analysis and basaltic geochemistry: *Geochemistry, Geophysics, Geosystems*, v. 19, no. 1, p. 175–213, <https://doi.org/10.1002/2017GC007251>.
- Mulder, J.A., Karlstrom, K.E., Fletcher, K., Heizler, M.T., Timmons, J.M., Crossey, L.J., Gehrels, G.E., and Pecha, M., 2017, The syn-orogenic sedimentary record of the Grenville Orogeny in southwest Laurentia: *Precambrian Research*, v. 294, p. 33–52, <https://doi.org/10.1016/j.precamres.2017.03.006>.
- Müller, R.D., Lim, V.S.L., and Isern, A.R., 2000, Late Tertiary tectonic subsidence on the northeast Australian passive margin: Response to dynamic topography?: *Marine Geology*, v. 162, p. 337–352, [https://doi.org/10.1016/S0025-3227\(99\)00089-4](https://doi.org/10.1016/S0025-3227(99)00089-4).
- Nilsen, T.H., and Stewart, J.H., 1980, The Antler orogeny—Mid-Paleozoic tectonism in western North America: *Geology*, v. 8, p. 298–303, [https://doi.org/10.1130/0091-7613\(1980\)8<298:TAOTIW>2.0.CO;2](https://doi.org/10.1130/0091-7613(1980)8<298:TAOTIW>2.0.CO;2).
- Noble, L.F., 1922, A section of the Paleozoic formations of the Grand Canyon at the Bass Trail: *U.S. Geological Survey Professional Paper 131-B*, p. B23–B73.
- Palmer, A.N., and Palmer, M.V., 1995, The Kaskaskia paleokarst of the northwestern Rocky Mountains and Black Hills, northwestern USA: Carbonates and Evaporites, v. 10, no. 2, p. 148–160, <https://doi.org/10.1007/BF03175400>.
- Parnell-Turner, R., White, N., Henstock, T., Murton, B., MacLennan, J., and Jones, S.M., 2014, A continuous 55-million-year record of transient mantle plume activity beneath Iceland: *Nature Geoscience*, v. 7, p. 914–919, <https://doi.org/10.1038/ngeo2281>.
- Parsons, B., and McKenzie, D., 1978, Mantle convection and the thermal structure of the plates: *Journal of Geophysical Research: Solid Earth*, v. 83, no. B9, p. 4485–4496, <https://doi.org/10.1029/JB083iB09p04485>.
- Parsons, B., and Sclater, J.G., 1977, An analysis of the variation of ocean floor bathymetry and heat flow with age: *Journal of Geophysical Research: Solid Earth and Planets*, v. 82, no. 5, p. 803–827, <https://doi.org/10.1029/JB082i005p00803>.
- Peirce, H.W., 1981, The Mississippian and Pennsylvanian (Carboniferous) systems in the United States—Arizona: *U.S. Geological Survey Professional Paper 1110-Z*, p. Z1–Z20.
- Petersen, K.D., Nielsen, S.B., Clausen, O.R., Stephenson, R., and Gerya, T., 2010, Small-scale mantle convection produces stratigraphic sequences in sedimentary basins: *Science*, v. 329, p. 827–830, <https://doi.org/10.1126/science.1190115>.
- Phipps Morgan, J., Morgan, W.J., Zhang, Y.S., and Smith, W.H.F., 1995, Observational hints for a plume-fed, suboceanic asthenosphere and its role in mantle convection: *Journal of Geophysical Research: Solid Earth*, v. 100, no. B7, p. 12,753–12,767, <https://doi.org/10.1029/95JB00041>.
- Poole, F.G., and Sandberg, C.A., 1977, Mississippian paleogeography and tectonics of the western United States, in *Proceedings, Pacific Coast Paleogeography Symposium 1*: Tulsa, Oklahoma, USA, Society of Economic Paleontologists and Mineralogists, p. 67–85.
- Priestley, K., and McKenzie, D., 2013, The relationship between shear wave velocity, temperature, attenuation and viscosity in the shallow part of the mantle: *Earth and Planetary Science Letters*, v. 381, p. 78–91, <https://doi.org/10.1016/j.epsl.2013.08.022>.
- Ramsbottom, W.H.C., and Saunders, W.B., 1985, Evolution and evolutionary biostratigraphy of Carboniferous ammonoids: *Journal of Paleontology*, v. 59, no. 1, p. 123–139.
- Ricard, Y., Richards, M., Lithgow-Bertelloni, C., and Le Stunff, Y., 1993, A geodynamic model of mantle density heterogeneity: *Journal of Geophysical Research: Solid Earth*, v. 98, no. B12, p. 21,895–21,909, <https://doi.org/10.1029/93JB02216>.
- Rice, C.L., 1984, Sandstone units of the Lee Formation and related strata in Eastern Kentucky: *U.S. Geological Survey Professional Paper 1151-G*, 62 p., <https://doi.org/10.3133/pp1151G>.
- Rice, C.L., 1985, Terrestrial vs. marine depositional model—A new assessment of subsurface lower Pennsylvanian rocks of southwestern Virginia: *Geology*, v. 13, p. 786–789, [https://doi.org/10.1130/0091-7613\(1985\)13<786:TVMDMN>2.0.CO;2](https://doi.org/10.1130/0091-7613(1985)13<786:TVMDMN>2.0.CO;2).
- Richards, F.D., Hoggard, M.J., and White, N.J., 2016, Cenozoic epeirogeny of the Indian peninsula: *Geochemistry, Geophysics, Geosystems*, v. 17, p. 4920–4954, <https://doi.org/10.1029/2016GC006545>.
- Richards, F.D., Hoggard, M.J., Cowton, L.R., and White, N.J., 2018, Reassessing the thermal structure of oceanic lithosphere with revised global inventories of basement depths and heat flow measurements: *Journal of Geophysical Research: Solid Earth*, v. 123, p. 9136–9161, <https://doi.org/10.1029/2018JB015998>.
- Richards, F.D., Hoggard, M.J., White, N.J., and Ghelichkhan, S., 2020, Quantifying the relationship between short-wavelength dynamic topography and thermomechanical structure of the upper mantle using calibrated parameterization of anelasticity: *Journal of Geophysical Research: Solid Earth*, v. 125, no. e2019JB019062, <https://doi.org/10.1029/2019JB019062>.
- Ritter, S.M., 1991, Conodont-based revision of Upper Devonian-Lower Pennsylvanian stratigraphy in the Lake Mead region of northwestern Arizona and southeastern Nevada: *Geology Studies*, v. 37, p. 125–138.
- Roberts, G.G., White, N.J., Martin-Brandis, G.L., and Crosby, A.G., 2012, An uplift history of the Colorado Plateau and its surroundings from inverse modeling of

- longitudinal river profiles: Tectonics, v. 31, no. TC4022, https://doi.org/10.1029/2012TC003107.
- Rooney, A.D., Austermann, J., Smith, E.F., Li, Y., Selby, D., Dehler, C.M., Schmitz, M.D., Karlstrom, K.E., and Macdonald, F.A., 2018, Coupled Re-Os and U-Pb geochronology of the Tonian Chuar Group, Grand Canyon: Geological Society of America Bulletin, v. 130, p. 1085–1098, https://doi.org/10.1130/B31768.1.
- Rose, E., 2006, Nonmarine aspects of the Cambrian Tonto Group of the Grand Canyon, USA, and broader implications: Paleoworld, v. 15, p. 223–241, https://doi.org/10.1016/j.palwo.2006.10.008.
- Rose, P.R., 1976, Mississippian carbonate shelf margins, western United States: Journal of Research of the U.S. Geological Survey, v. 4, no. 4, p. 449–466.
- Ross, C.A., and Ross, J.P., 1985, Late Paleozoic depositional sequences are synchronous and worldwide: Geology, v. 13, p. 194–197, https://doi.org/10.1130/0091-7613(1985)13<194:LPDAS>2.0.CO;2.
- Ross, C.A., and Ross, J.R.P., 1988, Late Paleozoic transgressive-regressive deposition, in Wilgus, C.K., Hastings, B.S., Ross, C.A., Posamentier, H., van Wagoner, J., and Kendall, C.G.St.C., eds., Sea-level changes—An integrated approach: Society of Economic Paleontologists and Mineralogists Special Publication 42, p. 227–247.
- Rudge, J.F., Shaw Champion, M.E., White, N., McKenzie, D., and Lovell, B., 2008, A plume model of transient diachronous uplift at the Earth's surface: Earth and Planetary Science Letters, v. 267, p. 146–160, https://doi.org/10.1016/j.epsl.2007.11.040.
- Saltzman, M.R., 2003, Late Paleozoic ice age: Oceanic gateway or pCO_2 ?: Geology, v. 31, no. 2, p. 151–154, https://doi.org/10.1130/0091-7613(2003)031<0151:LPIAOG>2.0.CO;2.
- Sando, W.J., 1974, Ancient solution phenomena in the Madison Limestone (Mississippian) of north-central Wyoming: Journal of Research of the U.S. Geological Survey, v. 2, no. 2, p. 133–141.
- Sando, W.J., 1985, Revised Mississippian time scale, western interior range, conterminous United States: U.S. Geological Survey Bulletin, v. 1605-A, p. A15–A26.
- Sando, W.J., 1988, Madison Limestone (Mississippian) paleokarst: A geologic synthesis, in James, N.P., and Choquette, P.W., Paleokarst: New York, Springer-Verlag, p. 278–305, https://doi.org/10.1007/978-1-4612-3748-8_13.
- Sando, W.J., Gordon, M.J., and Dutro, T.Jr., 1975, Stratigraphy and geologic history of the Amsden Formation (Mississippian and Pennsylvanian) of Wyoming: U.S. Geological Survey Professional Paper 848-A, 82 p., https://doi.org/10.3133/pp848A.
- Sando, W.J., Bamber, E.W., and Richards, B.C., 1990, The rugose coral *Ankhelesma*—Index to Viséan (Lower Carboniferous) shelf margin in the Western Interior of North America: U.S. Geological Survey Professional Paper 1895, p. B1–B29.
- Saunders, W.B., and Ramsbottom, W.H.C., 1986, The mid-Carboniferous eustatic event: Geology, v. 14, p. 208–212, https://doi.org/10.1130/0091-7613(1986)14<208:TME>2.0.CO;2.
- Schaeffer, A.J., and Lebedev, S., 2013, Global shear speed structure of the upper mantle and transition zone: Geophysical Journal International, v. 194, no. 1, p. 417–449, https://doi.org/10.1093/gji/ggt095.
- Sclater, J.G., and Christie, P.A.F., 1980, Continental stretching: an explanation of the post-mid-Cretaceous subsidence of the central North Sea basin: Journal of Geophysical Research: Solid Earth, v. 85, no. B7, p. 3711–3739, https://doi.org/10.1029/JB085iB07p03711.
- Shaw Champion, M.E., White, N.J., Jones, S.M., and Lovell, J.P.B., 2008, Quantifying transient mantle convective uplift: An example from the Faroe-Shetland Basin: Tectonics, v. 27, no. 1, https://doi.org/10.1029/2007TC002106.
- Shen, W., and Ritzwoller, M.H., 2016, Crustal and uppermost mantle structure beneath the United States: Journal of Geophysical Research: Solid Earth, v. 121, p. 4306–4342, https://doi.org/10.1002/2016JB012887.
- Shirley, D.H., 1988, Geochemical facies analysis of the Surprise Canyon Formation in Fern Glen Channelway, Central Grand Canyon, Arizona [M.S. dissertation]: Flagstaff, Arizona, USA, Northern Arizona University, 240 p.
- Siever, R., 1951, The Mississippian-Pennsylvanian unconformity in southern Illinois: American Association of Petroleum Geologists Bulletin, v. 35, no. 3, p. 542–581.
- Singer, A., Stanley, G.D., and Hinman, N.W., 2019, Anatomy of the Book Canyon conglomerate: A sequence boundary at the top of the Bear Gulch Limestone in the Big Snowy Trough: Facies, v. 65, article no. 15, https://doi.org/10.1007/s10347-019-0557-4.
- Skipp, B., 1969, Foraminifera, in McKee, E.D., and Gutschick, R.C., History of the Redwall Limestone of Northern Arizona: Geological Society of America Memoir 114, p. 173–256.
- Sleep, N., 1971, Thermal effects of the formation of Atlantic continental margins by continental break up: Geophysical Journal of the Royal Astronomical Society, v. 24, p. 325–350, https://doi.org/10.1111/j.1365-246X.1971.tb02182.x.
- Spasojevic, S., Liu, L., and Gurnis, M., 2009, Adjoint models of mantle convection with seismic, plate motion, and stratigraphic constraints: North America since the Late Cretaceous: Geochemistry, Geophysics, Geosystems, v. 10, no. 5, article no. Q05W02, https://doi.org/10.1029/2008GC002345.
- Steckler, M.S., and Watts, A.B., 1978, Subsidence of the Atlantic-type continental margin off New York: Earth and Planetary Science Letters, v. 41, no. 1, p. 1–13, https://doi.org/10.1016/0012-821X(78)90036-5.
- Stephenson, S.N., White, N.J., Carter, A., Seward, D., Ball, P.W., and Klöcking, M., 2021, Cenozoic dynamic topography of Madagascar: Geochemistry, Geophysics, Geosystems, v. 22, no. e2020GC009624, https://doi.org/10.1029/2020GC009624.
- Stucky de Quay, G., Roberts, G.G., Watson, J.S., and Jackson, C.A.-L., 2017, Incipient mantle plume evolution: Constraints from landscapes buried beneath the North Sea: Geochemistry, Geophysics, Geosystems, v. 18, no. 3, p. 973–993, https://doi.org/10.1002/2016GC006769.
- Sturmer, D.M., Trexler, J.H., Jr., and Cashman, P.H., 2018, Tectonic analysis of the Pennsylvania Ely-Bird Spring Basin: Late Paleozoic tectonism on the southwestern Laurentian Margin and the distal limit of the Ancestral Rocky Mountains: Tectonics, v. 37, p. 604–620, https://doi.org/10.1002/2017TC004769.
- Tidwell, W.D., Jennings, J.R., and Beus, S.S., 1992, A Carboniferous flora from the Surprise Canyon Formation in the Grand Canyon, Arizona: Journal of Paleontology, v. 66, no. 6, p. 1013–1021, https://doi.org/10.1017/S002336000020941.
- Timmons, J.M., Karlstrom, K.E., Dehler, C.M., Geissman, J.W., and Heizler, M.T., 2001, Proterozoic multistage (ca. 1.1 and 0.8 Ga) extension recorded in the Grand Canyon Supergroup and establishment of northwest- and north-trending grains in the southwestern United States: Geological Society of America Bulletin, v. 113, p. 163–181, https://doi.org/10.1130/0016-7606(2001)113<0163:PMCA>2.0.CO;2.
- Timmons, J.M., Karlstrom, K.E., Heizler, M.T., Bowring, S.A., Gehrels, G.E., and Crossey, L.J., 2005, Tectonic inferences from the ca. 1255–1100 Ma Unkar Group and Nankoweap Formation, Grand Canyon: Intracratonic deformation and basin formation during protracted Grenville orogenesis: Geological Society of America Bulletin, v. 117, p. 1573–1595, https://doi.org/10.1130/B25538.1.
- Timmons, J.M., Bloch, J., Fletcher, K., Karlstrom, K.E., Heizler, M., and Crossey, L.J., 2012, The Grand Canyon Unkar Group: Mesoproterozoic basin formation in the continental interior during supercontinent assembly, in Timmons, J.M., and Karlstrom, K.E., eds., Grand Canyon Geology: Two billion Years of Earth's History: Geological Society of America Special Paper 489, p. 25–48.
- Turner, C.E., 2003, Toroweap Formation, in Beus, S.S., and Morales, M., eds., Grand Canyon Geology (2nd edition): New York, USA, Oxford University Press, p. 180–195.
- van Wijk, J.W., Baldridge, W.S., van Hunen, J., Goes, S., Aster, R., Coblenz, D.D., Grand, S.P., and Ni, J., 2010, Small-scale convection at the edge of the Colorado Plateau: Implications for topography, magmatism, and evolution of Proterozoic lithosphere: Geology, v. 38, no. 7, p. 611–614, https://doi.org/10.1130/G31031.1.
- van Wijk, J.W., Koning, D., Axen, G., Coblenz, D., Gragg, E., and Sion, B., 2018, Tectonic subsidence, geoid analysis, and the Miocene-Pliocene unconformity in the Rio Grande rift, southwestern United States: Implications for mantle upwelling as a driving force for rift opening: Geosphere, v. 14, p. 684–709, https://doi.org/10.1130/GES01522.1.
- Vevers, J.J., and Powell, C.M., 1987, Late Paleozoic glacial episodes in Gondwanaland reflected in transgressive-regressive depositional sequences in Euramerica: Geological Society of America Bulletin, v. 98, p. 475–487, https://doi.org/10.1130/0016-7606(1987)98<475:LPGEIG>2.0.CO;2.
- Walker, R.T., Telfer, M., Kahle, R.L., Dee, M.W., Kahle, B., Schwenniger, J.L., Sloan, R.A., and Watts, A.B., 2016, Rapid mantle-driven uplift along the Angolan margin in the late Quaternary: Nature Geoscience, v. 9, p. 909–914, https://doi.org/10.1038/ngeo2835.
- Wang, W., and Bidgoli, T.S., 2019, Detrital zircon geochronologic constraints on patterns and drivers of continental-scale sediment dispersals and the Late Mississippian: Geochemistry Geophysics Geosystems, v. 20, p. 5522–5543, https://doi.org/10.1029/2019GC008469.
- Watts, A.B., 2001, Isostasy and flexure of the lithosphere: Cambridge, UK, Cambridge University Press.
- Webb, G.E., 1994, Paleokarst, paleosol, and rocky-shore deposits at the Mississippian-Pennsylvanian unconformity, northwestern Arkansas: Geological Society of America Bulletin, v. 106, p. 634–648, https://doi.org/10.1130/0016-7606(1994)106<0634:PPARSD>2.3.CO;2.
- Weil, A.B., Geissman, J.W., Heizler, M., and van der Voo, R., 2003, Paleomagnetism of middle Proterozoic mafic intrusions and upper Proterozoic (Nankoweap) red beds from the lower Grand Canyon supergroup, Arizona: Tectonophysics, v. 375, p. 199–220, https://doi.org/10.1016/S0040-1951(03)00339-1.
- Wessel, P., Luis, J.F., Uieda, L., Scharrer, R., Wobbe, F., Smith, W.H.F., and Tian, D., 2019, The Generic Mapping Tools Version 6: Geochemistry, Geophysics, Geosystems, v. 20, p. 5556–5564, https://doi.org/10.1029/2019GC008515.
- White, N., and Lovell, B., 1997, Measuring the pulse of a plume with the sedimentary record: Nature, v. 387, p. 888–891, https://doi.org/10.1038/43151.
- Wilson, M., and Downes, H., 2006, Tertiary-Quaternary intra-plate magmatism in Europe and its relationship to mantle dynamics, in Gee, D.G., and Stephenson, R., eds., European Lithosphere Dynamics: Geological Society, London, Memoir 32, p. 147–166, https://doi.org/10.1144/GSL.MEM.2006.032.01.09.
- Woods, A.D., 2009, Anatomy of an anachronistic carbonate platform: Lower Triassic carbonates of the southwestern Unites States: Australian Journal of Earth Sciences, v. 56, no. 6, p. 825–839, https://doi.org/10.1080/0812090903002649.
- Yuen, D.A., and Fleitout, L., 1985, Thinning of the lithosphere by small-scale convective destabilization: Nature, v. 313, p. 125–128, https://doi.org/10.1038/313125a0.
- Zoback, M.L., Anderson, R.E., and Thompson, G.A., 1981, Cainozoic evolution of the state of stress and style of tectonism of the Basin and Range Province of the western Unites States: Philosophical Transactions of the Royal Society of London Series A: Mathematical, Physical, and Engineering Sciences, v. 300, p. 407–434, https://doi.org/10.1098/rsta.1981.0073.

SCIENCE EDITOR: BRAD S. SINGER
ASSOCIATE EDITOR: ALAN ROONEY

MANUSCRIPT RECEIVED 7 DECEMBER 2020
REVISED MANUSCRIPT RECEIVED 11 MAY 2021
MANUSCRIPT ACCEPTED 22 JUNE 2021

Printed in the USA